

MULTIPLE SCALE METHODS FOR OPTIMIZATION OF DISCRETIZED CONTINUOUS FUNCTIONS*

NICHOLAS J. E. RICHARDSON[†], NOAH MARUSENKO[‡], AND
MICHAEL P. FRIEDLANDER^{†‡}

Abstract. A multiscale optimization framework for problems over a space of Lipschitz continuous functions is developed. The method solves a coarse-grid discretization followed by linear interpolation to warm-start project gradient descent on progressively finer grids. Greedy and lazy variants are analyzed and convergence guarantees are derived that show the multiscale approach achieves provably tighter error bounds at lower computational cost than single-scale optimization. The analysis extends to any base algorithm with iterate convergence at a fixed rate. Constraint modification techniques preserve feasibility across scales. Numerical experiments on probability density estimation problems, including geological data, demonstrate speedups of an order of magnitude or better.

Key words. multiresolution analysis, continuous optimization, approximation theory

MSC codes. 65B99, 65D15, 90C59

1. Introduction. Optimization over function spaces arises in applications ranging from density estimation to signal reconstruction. We consider the general problem of optimizing an objective $\mathcal{L} : \mathcal{C} \rightarrow \mathbb{R}$ over continuous functions $f : \mathcal{D} \rightarrow \mathbb{R}$ defined on an 1-dimensional domain $\mathcal{D} \subseteq \mathbb{R}$:

$$(P) \quad \min_f \{ \mathcal{L}(f) \mid f \in \mathcal{C} \},$$

where $\mathcal{C} \subseteq \mathcal{F} := \{f : \mathcal{D} \rightarrow \mathbb{R} \mid f \text{ is continuous}\}$ is a constraint set.

The space of all continuous functions \mathcal{F} is too large to optimize directly. We therefore restrict $\mathcal{C} \subseteq \mathcal{F}$ to reduce the uncountably infinite dimensional problem in (P) to a countably infinite or finite problem amenable to computation. We focus on Lipschitz continuous solutions. This mild regularity condition holds automatically for continuous functions on compact domains and is needed to prove precise error bounds for our multiscale approach.

One common approach discretizes the problem over a finite grid:

$$(1.1) \quad \min_X \{ \tilde{\mathcal{L}}(x) \mid x \in \tilde{\mathcal{C}} \},$$

where the vector $x \in \mathbb{R}^I$ represents the function f evaluated on a set of grid points. The discretized objective $\tilde{\mathcal{L}}$ and constraint set $\tilde{\mathcal{C}}$ correspond to their continuous counterparts.

Any discretization raises the question; how fine should be the discretization? When we have discretization choices to make, we often favor finer grids for accuracy. When data arrives pre-discretized, we prefer to incorporate all available information. Fine discretizations, however, carry computational costs: most operations are slower and consume more memory as problem size grows, often superlinearly, such as with matrix-matrix multiplication [23]. We propose a multiresolution approach that achieves faster convergence on fine-scale problems. Our method is inspired by wavelets [3] and multigrid [25] methods, and optimizes f over progressively finer discretizations.

*This work was funded by the Natural Sciences and Engineering Research Council of Canada. Manuscript Date: March 3, 2026.

[†]Department of Mathematics, University of British Columbia, Vancouver, BC, Canada

[‡]Department of Computer Science, University of British Columbia, Vancouver, BC, Canada

1.1. Related Work. Many approaches exist for optimizing over function spaces beyond simple discretizations. One class of methods restricts \mathcal{C} to a Hilbert space with basis functions $\{f_k\}$ and solves for optimal weights $\{a_k\}$ in the representation $f(v) = \sum_k a_k f_k(v)$. Examples include Fourier features, wavelets [3], and Legendre polynomials [24]. The calculus of variations provides an analytical framework for optimizing functionals, typically integrals involving the input function [9].

Finite parametrization offers another approach, exemplified by finding the mean μ and variance σ^2 in the family of normal distributions [26], or optimizing over weights $\{W_k\}$ and biases $\{b_l\}$ in fully connected neural networks [12]. Non-parametric methods such as kernel density estimation [5] and Gaussian mixture models [28] provide yet another alternative. Finally, convex duality techniques transform infinite-dimensional problems into finite-dimensional counterparts [6].

We focus on uniformly spaced discretizations: the approach is simple, used across a variety of settings, easy to implement and analyze, and sufficient in practice and theory for Lipschitz functions. More sophisticated discretization schemes have been well studied in differential equations [22], probability density estimation [4], machine learning [19], and approximation theory [24]. These schemes concentrate the grid where f exhibits larger variations (for differentiable f , where the gradient magnitude is larger) or near domain endpoints. Many results in this paper extend to such alternative discretization schemes.

Our method synthesizes ideas from wavelets [3], multigrid methods for partial differential equations [25], and multiresolution matrix factorization [10, 14]. At each scale s , we solve a distinct optimization problem (P_s) that discretizes the continuous problem (P) . Both the vector's dimension I and the objective function $\tilde{\mathcal{L}}_s$ adapt to the scale: a coarse-scale objective involves fewer summands, different grid points, and modified constraints. This differs from approaches that merely subsample variables while keeping the objective structure fixed. By re-discretizing both the domain and the objective at each scale, our framework ensures that each subproblem P_s properly approximates the continuous problem, not just its reduced fine-scale version. This contrasts more direct translations of multigrid for smooth optimization problems like MGProx [2] which uses a V-cycle to start with the finest scale problem and transfer information to the coarsest scale before working back to the finest scale problem. Our approach starts with the coarsest scale and only works towards the finest scale problem. We also study a more general problem that does not rely on a specific inner algorithm.

Each resolution level provides a warm start for the next finer scale, typically with a smaller error than random initialization. Warm-start strategies appear throughout numerical optimization, from stochastic gradient descent [16] to first-order methods [1].

Our coarse-scale optimization updates only a subset of coordinates (the free variables present at the current resolution) while finer-scale variables remain implicit. This connects to coordinate-wise optimization methods, including greedy descent [8], coordinate descent [17], and block coordinate decent [27].

1.2. Contributions. We develop multiscale methods for optimizing over spaces of Lipschitz functions and establish the first theoretical framework for multiscale optimization in this setting. We propose two variants: a *greedy* approach that re-optimizes all variables at each scale (Algorithm 2.1 and subsection 4.2), and a *lazy* approach that freezes coarse-scale values and optimizes only newly interpolated points (Algorithm 2.1 and subsection 4.3). Both variants achieve faster convergence to tighter error bounds than gradient descent on a single fine discretization (Corollaries 6.5 and 6.8). The analysis extends to any optimization algorithm with iterate convergence

at a fixed rate (Definition 2.5). We further develop constraint modification techniques that preserve feasibility across scales (section 3), and bound the error between our algorithm output and the solution to the continuous problem (section 5). Numerical tests illustrate the effectiveness of the multiscale approach on synthetic (subsections 2.3 and 7.2) and realworld (subsection 7.3) data for a distribution de-mixing problem. We make clear that although the theoretical analysis is given to solve 1-dimensional problems, the general principle extends to higher dimensions where the objective variable becomes one or more tensors (section 7).

1.3. Reproducible research. The data files and scripts used to generate the numerical results presented in this paper are available from the GitHub repository [21].

2. The Multiscale Optimization Method. We introduce the multiscale method through a concrete example that demonstrates how it can exploit problem structure across discretization scales to reduce overall computation cost.

2.1. Motivating Example. Consider recovering a smooth probability density function from polynomial measurements. We formulate this as an inverse least-squares problem over differentiable densities p on $\mathcal{D} = [-1, 1]$:

$$\min_p \left\{ \frac{1}{2} \|\mathcal{A}(p) - y\|_2^2 + \frac{1}{2} \lambda \|p'\|_2^2 \mid \|p\|_1 = 1 \text{ and } p \geq 0 \right\},$$

where the constraints ensure p is a valid probability density. The measurement operator \mathcal{A} maps p to an M -vector with elements

$$\mathcal{A}(p)[m] = \langle a_m, p \rangle \quad \text{for } m = 1, \dots, M,$$

with normalized Legendre polynomials $a_m(t) = \left(\frac{2m+1}{2}\right)^{1/2} \sum_{k=0}^m \binom{m}{k} \binom{m+k}{k} \left(\frac{t-1}{2}\right)^k$. The regularization term $\|p'\|_2^2 = \int_{-1}^1 (p'(t))^2 dt$ encourages smoothness in the recovered density. We discretize this continuous problem on a uniform grid to obtain

$$(2.1) \quad \min_{x_1} \left\{ \frac{1}{2} \|A_1 x_1 - y\|_2^2 + \frac{1}{2} \lambda x_1^\top G_1 x_1 \mid \|x_1\|_1 = 1 \text{ and } x_1 \geq 0 \right\},$$

where the vector $x_1 = (x_1[1], x_1[2], \dots, x_1[I_1])$ represents the uniform discretization of p on $[-1, 1]$ at the finest scale with grid spacing $\Delta t_1 = 2/(I_1 - 1)$:

$$x_1[i] = p(t_1[i]) \Delta t_1, \quad \text{with } t_1[i] = -1 + 2 \frac{i-1}{I_1-1}.$$

The discretized measurement operator A_1 and graph Laplacian G_1 , which approximates the second derivative operator, are

$$A_1[m, i] = a_m(t_1[i]) \quad \text{and} \quad G_1 = \frac{1}{\Delta t_1^3} \begin{bmatrix} 1 & -1 & & & \\ -1 & 2 & -1 & & \\ & \ddots & \ddots & \ddots & \\ & & -1 & 2 & -1 \\ & & & -1 & 1 \end{bmatrix}.$$

We return to this example in subsection 2.2, after introducing the general multiscale framework, to demonstrate how the method applies to this specific problem.

2.2. Method Overview. We solve the continuous optimization problem (P) via progressive grid refinement. Starting from a coarse discretization, we solve the discretized problem at each scale, interpolate the solution to the next finer grid, and use it to warm-start the optimization. Algorithm 2.1 formalizes this refinement process.

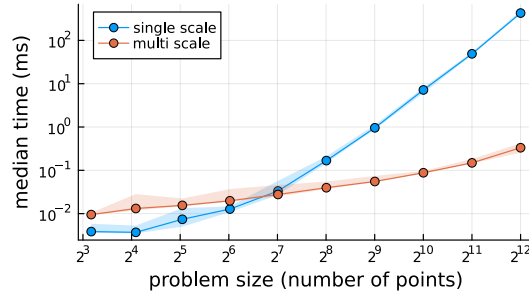


Fig. 1: Comparison of multiscale vs single-scale approach for the motivating example from subsection 2.1. Dots represent the median total time in milliseconds over 100 trials; shaded regions represent the 5th and 95th percentile times. The multiscale approach improves algorithm speed over a single scaled approach once the problem size is large enough. Details are provided in subsection 2.3.

We index discretization levels by a *scale* parameter s , where $s = 1$ denotes the finest discretization and increasing s corresponds to progressively coarser grids. At scale s , the discretized problem becomes

$$(P_s) \quad \min_{x_s} \{ \tilde{\mathcal{L}}_s(x_s) \mid x_s \in \tilde{\mathcal{C}}_s \},$$

where $x_s \in \mathbb{R}^{I_s}$, and $\tilde{\mathcal{L}}_s$ and $\tilde{\mathcal{C}}_s$ denote the discretized objective and constraint set.

We return to the motivating example from subsection 2.1 to demonstrate how the general framework applies. Recall that we recover a probability density from Legendre polynomial measurements, discretized at the finest scale as (2.1). At scale s , the discretized problem becomes

$$(2.2) \quad \min_{x_s} \left\{ \frac{1}{2} \|A_s x_s - y\|_2^2 + \frac{1}{2} \lambda x_s^\top G_s x_s \mid \|x_s\|_1 = 2^{1-s} \text{ and } x_s \geq 0 \right\}$$

where x_s is an $I_s = 2^{s-1} + 1$ vector that discretizes p at scale s with grid spacing $\Delta t_s = 2^{s-1} \Delta t_1$. The constraint $\|x_s\|_1 = 2^{1-s}$ scales with the grid spacing to preserve the continuous constraint $\int p(t) dt = 1$ across all scales (see section 3). The scaled measurement operator A_s and graph Laplacian G_s are defined as

$$A_s = 2^{s-1} A_1[:, 1 : 2^{s-1} : I_1] \quad \text{and} \quad G_s = 2^{1-s} G_1[1 : 2^{s-1} : I_1, 1 : 2^{s-1} : I_1],$$

where the slicing notation $1 : 2^{s-1} : I_1$ selects every (2^{s-1}) -th point from the finest grid. The prefactors 2^{s-1} and 2^{1-s} ensure the two main quantities in the loss remain balanced at each scale:

$$A_s x_s \approx A_1 x_1 \quad \text{and} \quad x_s^\top G_s x_s \approx x_1^\top G_1 x_1.$$

This balancing ensures each scaled problem is regularized similarly by λ .

2.3. Motivating Example: Numerics. To emphasise the concepts behind multiscale, we compare an instance of the multiscale method (see Algorithm 2.1) against single scale optimization on the motivating example from subsection 2.1. Additional numerics and details are provided in sections SM2 and 7.

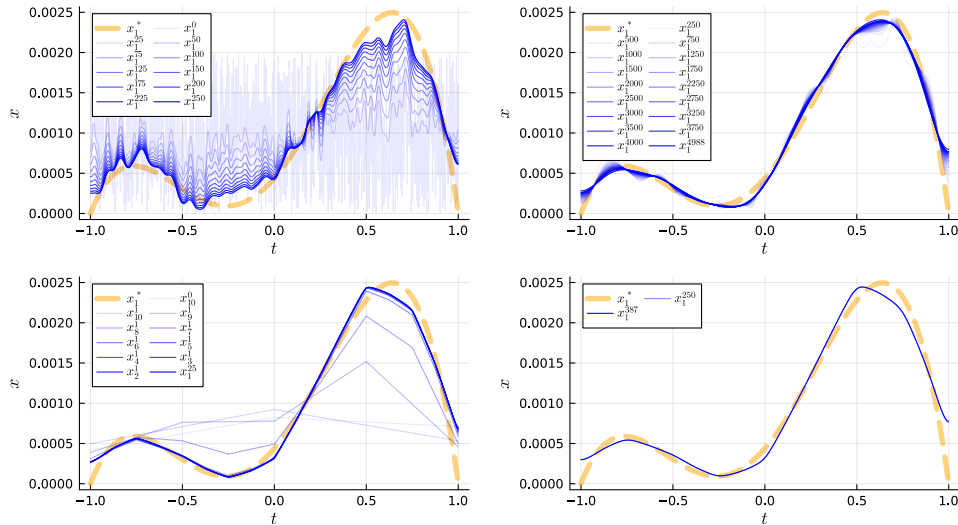


Fig. 2: Typical progression of iterates x_s^k for scale s and iteration k using single scale (top row) and multiscale (bottom row) approaches for the motivating example from subsection 2.1. The clean ground truth is plotted behind in the thick dashed lined.

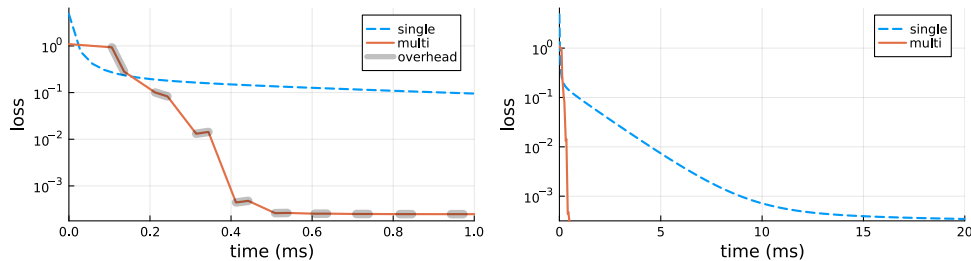


Fig. 3: Typical loss convergence using single scale (dashed blue) and multiscale (solid orange) approaches for the motivating example from subsection 2.1. The left plot shows the first millisecond, and the right plot shows the first 20 milliseconds. The left plot also highlights in grey regions that are not from projected gradient descent steps. These are the result of minimal overhead with the multiscale method such as interpolation, allocations, and extra function calls.

Figure 1 illustrates the improvement in computation time versus problem size achieved by the multiscale approach. Figure 2 shows the typical convergence of iterates x_s^k for single scale and multiscale approaches. And Figure 3 shows the typical loss convergence for the single scale and multiscale methods.

We call multiscale’s tendency to smooth iterates an implicit regularization. This helps smooth solutions by carrying information from farther away points to speed up convergence. In this problem, the graph laplacian regularizer only looks at the immediate neighbouring points. So working at coarser scales lets us compare points that are not immediately neighbouring at the finest scale.

2.4. Descritization, Coarsening, and Interpolation. Unless otherwise stated, we restrict the focus of this paper to scalar functions $f : [\ell, u] \rightarrow \mathbb{R}$ on the 1-dimensional domain $\mathcal{D} = [\ell, u]$ with uniform discretization

$$x_s[i] = f(t_s[i]), \quad \text{with} \quad t_s[i] = \ell + \frac{i-1}{I_s-1}(u - \ell).$$

This specialization simplifies our exposition and is without loss of generality because the multiscale framework extends to tensor-valued functions by vectorizing $X_s \in \mathbb{R}^{I_1 \times \dots \times I_N}$ as $x_s \in \mathbb{R}^{I_1 \dots I_N}$ and adapting interpolation operators accordingly. Section 7 demonstrates this extension.

The multiscale framework requires operators to transfer solutions of (P_s) between scales and to eventually construct approximate solutions to the continuous problem (P) . Any coarsening and interpolation method could be used, including splines [7] and Chebyshev and Lagrange polynomials [24]. We focus on dyadic coarsening, which keeps every second point, and midpoint linear interpolation. These are defined below. Figure 4 illustrates this discretization hierarchy and midpoint interpolation scheme.

DEFINITION 2.1 (Dyadic Coarsening). *Dyadic coarsening maps a vector $x \in \mathbb{R}^I$ to $\bar{x} \in \mathbb{R}^{\lfloor (I+1)/2 \rfloor}$ by selecting odd-indexed entries:*

$$\bar{x}[i] = x[2i - 1], \quad i = 1, \dots, \lfloor (I + 1)/2 \rfloor.$$

DEFINITION 2.2 (Midpoint Linear Interpolation). *Midpoint linear interpolation inserts a linearly interpolated point between each adjacent pair of entries in $x \in \mathbb{R}^I$ to produce $\underline{x} \in \mathbb{R}^{2I-1}$:*

$$\underline{x}[i] = \begin{cases} x[\frac{i+1}{2}] & \text{if } i \text{ is odd,} \\ \frac{1}{2} (x[\frac{i}{2}] + x[\frac{i}{2} + 1]) & \text{if } i \text{ is even.} \end{cases}$$

The operators in the coarsening and interpolation definitions translate between scales s with the notation

$$\bar{x}_s = x_{s+1} \quad \text{and} \quad \underline{x}_s = x_{s-1}.$$

The overline operator $\bar{(\cdot)}$ maps x_s to the coarser scale $s + 1$; the underline operator $\underline{(\cdot)}$ maps to the finer scale $s - 1$; see Figure 4.

When analyzing the multiscale algorithm, we need to refer to the newly added interpolated points. We call this vector the *free variables* $x_{(s)}$, a term justified in subsection 2.5.

DEFINITION 2.3 (Vector of Free Variables). *Given the (I_{s+1}) -vector x_{s+1} and its interpolation $\underline{x}_{s+1} = x_s$, the $(I_{s+1} - 1)$ -vector of free variables has entries*

$$x_{(s)}[i] = \frac{1}{2}(x_{s+1}[i] + x_{s+1}[i + 1]), \quad i = 1, \dots, I_{s+1} - 1.$$

These are the newly added points in x_s when interpolating x_{s+1} . At the coarsest scale $s = S$, we set $x_{(S)} = x_S$.

To convert a discrete solution x_1 of (P_s) at the finest scale $s = 1$ to an approximate solution to the continuous problem (P) , we define a piecewise linear approximation. This approximation stitches secants through (possibly approximate) sample points [7].

DEFINITION 2.4 (Piecewise Linear Approximation). *Let the I -vector x represent (possibly approximate) samples of a function f at locations $t_1 < \dots < t_I$. The piecewise linear approximation constructed from x is*

$$\hat{f}_x(t) = \frac{x[i+1] - x[i]}{t_{i+1} - t_i}(t - t_i) + x[i] \quad \text{where} \quad t_i \leq t \leq t_{i+1} \quad \text{for} \quad i = 1, \dots, I.$$

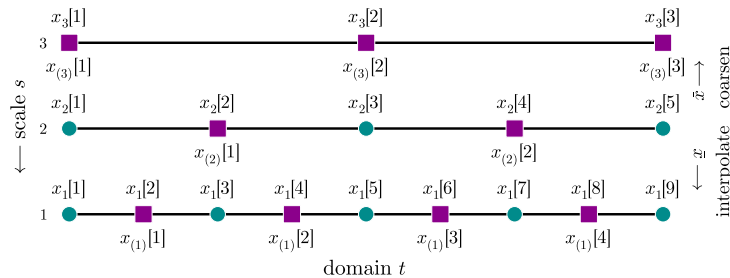


Fig. 4: Discretization of an interval with $S = 3$ scales. Each scale s has $2^{S-s+1} + 1$ points. Starting at scale $s = 3$, newly added points at each scale (the free variables $x_{(s)}[i]$) are shown in purple squares, while existing points are shown in teal circles.

REMARK 1. The subscript in \hat{f}_x identifies the vector x that defines the approximation. When x contains samples from a function, that is, $x[i] = f(t_i)$, we omit the subscript and write $\hat{f}(t)$.

2.5. Greedy and Lazy Multiscale Algorithms. We present two variants of the multiscale method (Algorithm 2.1) outlined in subsection 2.2 for solving (P): the *greedy* variant, which optimizes all grid points at each scale, and the *lazy* variant, which optimizes only the newly interpolated points at each finer scale. Both variants apply an update rule $x^{k+1} = U(x^k)$ at each scale, and our convergence analysis holds for any such update rule that achieves q -linear iterate convergence.

DEFINITION 2.5 (q -Linear Iterate Convergence). An iterative algorithm with update rule $x^{k+1} = U(x^k)$ has global q -linear iterate convergence with rate $q \in [0, 1)$ when

$$\|x^k - x^*\|_2 \leq (q)^k \|x^0 - x^*\|_2$$

for any initialization $x^0 \in \tilde{\mathcal{C}}$ and minimizer x^* of $\tilde{\mathcal{L}}(x)$ over $\tilde{\mathcal{C}}$ that may depend on x^0 .

Our software implementation (section 7), uses projected gradient descent as the update rule, which is described by

$$(2.3) \quad x^{k+1} \leftarrow U(x^k) = P_{\tilde{\mathcal{C}}}(x^k - \alpha \nabla \tilde{\mathcal{L}}(x^k))$$

where $P_{\tilde{\mathcal{C}}}(x) = \operatorname{argmin} \{ \|x - y\|_2 \mid y \in \tilde{\mathcal{C}} \}$ denotes the projection of x onto $\tilde{\mathcal{C}}$. The standard analysis gives the following q -linear rate for strongly-convex objectives.

LEMMA 2.6 (Descent Lemma [18, Theorem 2.1.15]). Projected gradient descent with stepsize $0 < \alpha \leq 2/(\mathcal{S}_{\tilde{\mathcal{L}}} + \mu_{\tilde{\mathcal{L}}})$ has iterate convergence with rate

$$q(\alpha) = \sqrt{1 - \frac{2\alpha\mathcal{S}_{\tilde{\mathcal{L}}}\mu_{\tilde{\mathcal{L}}}}{\mathcal{S}_{\tilde{\mathcal{L}}} + \mu_{\tilde{\mathcal{L}}}}}.$$

This is minimized at a stepsize of $\alpha = 2/(\mathcal{S}_{\tilde{\mathcal{L}}} + \mu_{\tilde{\mathcal{L}}})$, where we obtain the iterate convergence $q(\alpha) = (c - 1)/(c + 1)$ for a condition number of $c = \mathcal{S}_{\tilde{\mathcal{L}}}/\mu_{\tilde{\mathcal{L}}}$.

Although we can prescribe the number of iterations K_s at each scale in advance, in practice we may also use additional convergence criteria (such as a small gradient) at each scale in addition to this predetermined maximum.

Algorithm 2.1 The Multiscale Method: step 6 specifies Greedy or Lazy versions

- 1: Randomly initialize x_s^0 at the coarsest scale $s = S$.
 - 2: Perform K_s iterations of projected gradient descent on x_s^0 to approximately solve (P_s) at scale $s = S$ and obtain $x_s^{K_s}$.
 - 3: **for** scales $s = S - 1, S - 2, \dots, 1$ **do**
 - 4: Interpolate $x_{s+1}^{K_{s+1}}$ to obtain $\underline{x}_{s+1}^{K_{s+1}}$ according to Definition 2.2.
 - 5: Initialize the next finest scale $x_s^0 = \underline{x}_{s+1}^{K_{s+1}}$ using the previous scale's interpolated solution.
 - 6: Perform K_s iterations of projected gradient descent (2.3) on x_s^0 (Greedy) or $x_{(s)}^0$ (Lazy) to approximately solve (P_s) at scale s and obtain $x_s^{K_s}$.
 - 7: **end for**
 - 8: **return** Approximate solutions $x_1^{K_1}$ and $\hat{f}_{x_1^{K_1}}$ for (P_s) at $s = 1$ and (P) respectively.
-

3. Discretizing Constraints. The multiscale approach requires discretizing (P) at multiple scales. Given a discretization of the continuous constraint \mathcal{C} from (P) to the finest scale $\tilde{\mathcal{C}}_1$ in (P_s) , we must determine the appropriate discretized constraint sequence $\tilde{\mathcal{C}}_s$ at coarser scales $s = S - 1, S - 2, \dots, 1$.

Pointwise constraints $\mathcal{C} = \{f : \mathcal{D} \rightarrow \mathbb{R} \mid f(t) \in \mathcal{X}\}$ transfer verbatim to any scale: $\tilde{\mathcal{C}}_s = \{x_s \in \mathbb{R}^{I_s} \mid x[i] \in \mathcal{X}\}$. However, linear and moment constraints require careful scaling to maintain consistency across discretization levels.

Consider a p -norm constraint on f :

$$\mathcal{C} = \left\{ f : \mathcal{D} \rightarrow \mathbb{R} \mid \|f\|_p = c \right\}.$$

The natural discretization $\tilde{\mathcal{C}}_1 = \{x_1 \in \mathbb{R}^{I_1} \mid \|x_1\|_p = c\}$ correctly approximates \mathcal{C} when we scale the entries of x_1 by the grid size: $x_1[i] = f(t_1[i])(\Delta t)^{1/p}$. With this scaling, the discrete norm approximates the continuous norm:

$$c^p = \|x_1\|_p^p = \sum_{i=1}^{I_1} f(t_1[i])^p \Delta t \approx \int_{\mathcal{D}} f(t)^p dt = \|f\|_p^p,$$

as $I_1 \rightarrow \infty$. At coarse scale s , we modify the constraint to

$$\tilde{\mathcal{C}}_s = \left\{ x_s \in \mathbb{R}^{I_s} \mid \|x_s\|_p = c \cdot (I_s/I_1)^{1/p} \right\}.$$

This scaling preserves the constraint across scales. The Lipschitz property of f ensures neighboring entries in x_s remain similar, so

$$c^p = \frac{I_1}{I_s} \|x_s\|_p^p = \frac{I_1}{I_s} \sum_{i=1}^{I_s} (x_s[i])^p \approx \sum_{i=1}^{I_1} (x_1[i])^p = \|x_1\|_p^p.$$

Linear constraints require analogous scaling. For L_{g_k} -Lipschitz functions $g_k : \mathcal{D} \rightarrow \mathbb{R}$, the continuous constraint

$$\mathcal{C} = \{ f : \mathcal{D} \rightarrow \mathbb{R} \mid \langle g_k, f \rangle = b[k], k \in [K] \} \quad \text{where } b \in \mathbb{R}^K,$$

discretizes at scale s as

$$\tilde{\mathcal{C}}_s = \{ x_s \in \mathbb{R}^{I_s} \mid A_s x_s = b \cdot (I_s/I_1) \},$$

where $A_s[k, i] = g_k(t_s[i])(\Delta t)^{1/2}$ and $x_s[i] = f(t_s[i])(\Delta t)^{1/2}$.

We bound the discretization error to justify our constraint modification across scales. To do this, we extend of the definition of Lipschitz continuity to vectors.

DEFINITION 3.1 (Lipschitz Vector). A vector $x \in \mathbb{R}^I$ is L_x -Lipschitz when,

$$|x[i] - x[j]| \leq L_x |i - j| \quad \text{for all } i, j \in [I].$$

We also get a correspondence between Lipschitz functions and vectors.

COROLLARY 3.2 (Lipschitz Vectors and Functions). Given I samples $x[i] = f(t[i])$ of an L_f -Lipschitz function $f : \mathbb{R} \rightarrow \mathbb{R}$ on a uniformly spaced grid $\{t[i]\}$, the vector $x \in \mathbb{R}^I$ is $L_x = L_f \Delta t$ Lipschitz.

Proof. Let $i, j \in [I]$. Our grid has points $t[i] = l + (i - 1)\Delta t$, so we have

$$|x[i] - x[j]| = |f(t[i]) - f(t[j])| \leq L_f |t[i] - t[j]| = L_f \Delta t |i - j|. \quad \square$$

The following proposition quantifies how linear constraints transform under coarsening.

PROPOSITION 3.3 (Single Linear Constraint Scaling). Let $a \in \mathbb{R}^I$ discretize a bounded L_g -Lipschitz function $g : [\ell, u] \rightarrow \mathbb{R}$, and let x discretize a bounded L_f -Lipschitz function f . Define the Lipschitz constant for the product function fg as $L_{fg} = L_f \|g\|_\infty + L_g \|f\|_\infty$. If $\langle a, x \rangle = b$, then

$$\begin{aligned} |\langle \bar{a}, \bar{x} \rangle - \frac{1}{2}b| &\leq \frac{1}{4}L_{fg}(u-l)\frac{I}{I-1} \quad \text{for even } I, \\ |\langle \bar{a}, \bar{x} \rangle - \frac{1}{2}\frac{I+1}{I}b| &\leq \frac{1}{2}L_{fg}(u-l) \quad \text{for odd } I. \end{aligned}$$

Proof. See subsection A.1. □

Proposition 3.3 extends naturally to multiple linear constraints, as described in the following corollary.

COROLLARY 3.4 (Matrix Linear Constraint Scaling). Let $g_k : [\ell, u] \rightarrow \mathbb{R}$ be bounded L_{g_k} -Lipschitz functions for $k \in [K]$. Let $A \in \mathbb{R}^{K \times I}$ be the discretization $A[k, i] = g_k(t[i])$, and define $\bar{A} = A[:, \text{begin} : 2 : \text{end}]$ as the $(K \times \lceil I \rceil_e / 2)$ -submatrix with every other column removed, where $\lceil I \rceil_e$ rounds up to the nearest even integer. Define $L_{fg} = \max_{k \in [K]} (L_{fg_k}) = \max_{k \in [K]} (L_f \|g_k\|_\infty + L_{g_k} \|f\|_\infty)$ as the maximum Lipschitz constant of the product functions $\{fg_k\}_{k \in [K]}$. If $Ax = b \in \mathbb{R}^K$, then

$$\begin{aligned} \|\bar{A}\bar{x} - \frac{1}{2}b\|_2 &\leq \sqrt{K} \cdot \frac{1}{4}L_{fg}(u-l)\frac{I}{I-1} \quad \text{for even } I, \\ \|\bar{A}\bar{x} - \frac{I+1}{2I}\frac{1}{2}b\|_2 &\leq \sqrt{K} \cdot \frac{1}{2}L_{fg}(u-l) \quad \text{for odd } I. \end{aligned}$$

Proof. Let $a_k = A[k, :] \in \mathbb{R}^I$ be the k th row vector in A . By Proposition 3.3,

$$\begin{aligned} \|\bar{A}\bar{x} - \frac{b}{2}\|_2^2 &= \sum_{k=1}^K \left| \langle \bar{a}_k, \bar{x} \rangle - \frac{b[k]}{2} \right|^2 \leq \sum_{k=1}^K \left(\frac{I}{I-1} \frac{L_{fg_k}(u-l)}{4} \right)^2 \\ &\leq \left(\frac{I}{I-1} \frac{u-l}{4} \right)^2 \sum_{k=1}^K \max_k \{(L_{fg_k})^2\} = \left(\frac{I}{I-1} \frac{u-l}{4} \right)^2 (L_{fg})^2 K, \end{aligned}$$

for even I . Taking square roots completes this case, and the case for odd I is similar. □

The 1-norm constraint admits analogous scaling bounds.

PROPOSITION 3.5 (L1-norm Constraint Scaling). Let $x \in \mathbb{R}^I$ discretize a bounded L_f -Lipschitz function f . If $\|x\|_1 = b$, then the coarsened constraint satisfies the bounds

$$\begin{aligned} \|\bar{x}\|_1 - \frac{1}{2}b &\leq \frac{1}{4}L_f(u-l)\frac{I}{I-1} \quad \text{for even } I, \\ \|\bar{x}\|_1 - \frac{I+1}{I}\frac{1}{2}b &\leq \frac{1}{2}L_f(u-l) \quad \text{for odd } I. \end{aligned}$$

Proof. The proof is similar to the proof of Proposition 3.3 (see subsection A.1) by considering the vector $a = \text{sign}(x)$, and using the Lipschitz constant L_f for f to bound $|x[i] - x[i + 1]|$ in place of L_{fg} . \square

Proposition 3.5 specializes to a clean asymptotic behavior in the normalized case. For $z = x/\|x\|_1$, the bound for even I becomes

$$\left| \|\bar{z}\|_1 - \frac{1}{2} \right| \leq \frac{1}{4b} L_f (u - l) \frac{I}{I-1}.$$

As the discretization refines ($I \rightarrow \infty$), we have $b = \|x\|_1 \rightarrow \infty$, so the bound vanishes and $\|\bar{z}\|_1 \rightarrow 1/2$. The same limit holds for odd I , and also extends to other p -norms.

4. Convergence of a Multiscale Method. Both the standard and multiscale approaches converge because, by design, they both apply a convergent algorithm at the finest scale. The multiscale approach achieves faster convergence by warm starting the fine-scale iterations with solutions from coarser scales. The next subsections develop this analysis.

Subsection 4.1 establishes tight bounds on the error between smooth and strongly convex Lipschitz functions and their linear interpolation. Subsection 4.2 proves convergence when we solve the problem along the entire new discretization at each scale. Subsection 4.3 proves convergence when we freeze previously computed points and solve only at the newly interpolated points for each scale.

4.1. Functional Analysis Lemmas. To analyze multiscale method convergence, we first establish bounds on discretizing Lipschitz functions and approximating them with linear interpolations. We focus on solving the discretized problem (P_s) in one dimension with any algorithm that achieves iterate convergence at the rate specified in Definition 2.5.

The following lemma provides the foundation for analyzing linear interpolations of Lipschitz functions and, ultimately, our multiscale algorithm.

LEMMA 4.1 (Lipschitz Function Interpolation). *Let $f : \mathbb{R}^N \rightarrow \mathbb{R}$ be L_f -Lipschitz. For all $a, b \in \mathbb{R}^N$ and $\lambda_1, \lambda_2 \geq 0$, $\lambda_1 + \lambda_2 = 1$, the error between f evaluated at a convex combination of a and b and the linear interpolation of $f(a)$ and $f(b)$ satisfies*

$$(4.1) \quad |f(\lambda_1 a + \lambda_2 b) - (\lambda_1 f(a) + \lambda_2 f(b))| \leq 2L_f \lambda_1 \lambda_2 \|a - b\|_2.$$

Proof. See subsection A.2 and Figure 5. \square

Since Lemma 4.1 is central to the analysis of linear interpolations of Lipschitz functions and ultimately our multiscale algorithm, we require a tight bound on the interpolation error. The bound in (4.1) is optimal among all bounds independent of the endpoint values $f(a)$ and $f(b)$, as demonstrated by the explicit construction in the proof of Lemma 4.2.

LEMMA 4.2 (Lipschitz Interpolation Tightness). *Given $\lambda_1, \lambda_2 \geq 0$ with $\lambda_1 + \lambda_2 = 1$, an interval $[\ell, u]$, and constant $L_f > 0$, there exists an L_f -Lipschitz function on $[\ell, u]$ such that (4.1) holds with equality.*

Proof. Construct $f(t) = L_f |t - (\lambda_1 \ell + \lambda_2 u)|$. This function is L_f -Lipschitz with end-point values $f(\ell) = L_f \lambda_2 |\ell - u|$ and $f(u) = L_f \lambda_1 |\ell - u|$, and $f(\lambda_1 \ell + \lambda_2 u) = 0$. Therefore $|\lambda_1 f(\ell) + \lambda_2 f(u) - f(\lambda_1 \ell + \lambda_2 u)| = 2L_f \lambda_1 \lambda_2 |\ell - u|$. \square

To bound the error introduced when interpolating a coarse-scale solution to a finer scale, we apply Lemma 4.1 repeatedly with centre point interpolation ($\lambda_1 = \lambda_2 = 1/2$). This bounds the error between an exact fine-scale discretization $x_s^*[j] = f(t_s[j])$ and

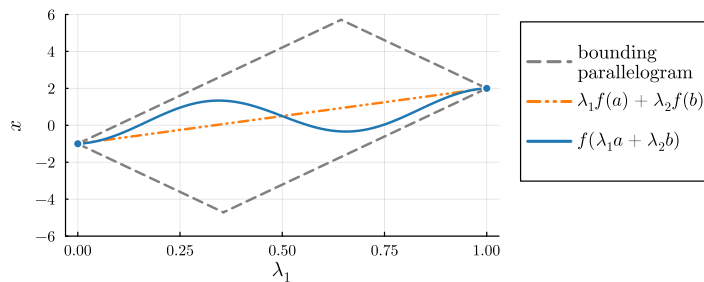


Fig. 5: Example for Lemma 4.1 with the function $x = f(t) = t - \cos(3\pi t)$ on the interval $[\ell, u] = [0, 1]$. The function f must lie within the dashed parallelogram since it is $L_f = 1 + 3\pi$ Lipschitz. Lemma 4.1 uses the parallelogram constraint to bound the distance between f and the linear interpolation $\lambda_1 f(a) + \lambda_2 f(b)$. Lemma 4.2 shows that the bound in (4.1) is tight for any given $\lambda_1, \lambda_2 \geq 0$ with $\lambda_1 + \lambda_2 = 1$.

the linear interpolation $x_s = \underline{x}_{s+1}$ obtained from a coarser discretization $x_{s+1}[i] = f(t_{s+1}[i])$. See Figure 6 (top).

LEMMA 4.3 (Exact Interpolation). *Let $f : [\ell, u] \rightarrow \mathbb{R}$ be L_f -Lipschitz continuous. On the interval $[\ell, u]$, let t_s be a fine grid with $J = 2I - 1$ points, and t_{s+1} be a coarse grid with I points. Discretize the function exactly at both scales to obtain vectors $x_s^* \in \mathbb{R}^J$ and $x_{s+1}^* \in \mathbb{R}^I$ where $x_s^*[j] = f(t_s[j])$ and $x_{s+1}^*[i] = f(t_{s+1}[i])$. Let $x_{s+1} = x_{s+1}^* \in \mathbb{R}^I$ and linearly interpolate to obtain $x_s = \underline{x}_{s+1} \in \mathbb{R}^J$ (see Definition 2.2). Then the difference between the interpolated x_s and exact values x_s^* is bounded by*

$$(4.2) \quad \|x_s - x_s^*\|_2 \leq L_f \frac{1}{2\sqrt{I-1}} |u - \ell|.$$

Proof. See subsection A.3. □

When the coarse discretization contains error, the interpolation analysis extends naturally. Suppose we interpolate not from exact values $x_{s+1}[i] = x_{s+1}^*[i] = f(t_{s+1}[i])$, but from *approximate values* $x_{s+1}[i] = x_{s+1}^*[i] + \delta[i] = f(t_{s+1}[i]) + \delta[i]$, where δ is an I -vector that represents the error at the coarse scale. Figure 6 (bottom) visualizes this scenario.

LEMMA 4.4 (Inexact Interpolation). *Consider the setup of Lemma 4.3 with one modification: the coarse discretization $x_{s+1} = x_{s+1}^* + \delta$ contains error $\delta \in \mathbb{R}^I$ before we interpolate to obtain $x_s = \underline{x}_{s+1}$. The difference between the interpolated values x_s and exact values x_s^* satisfies*

$$(4.3) \quad \|x_s - x_s^*\|_2 \leq \sqrt{2} \|\delta\|_2 + L_f \frac{1}{2\sqrt{I-1}} |u - \ell|.$$

Proof. See subsection A.4. □

This bound decomposes into two terms corresponding to distinct error sources. The first term captures the error from interpolating approximate values $x_{s+1} = x_{s+1}^* + \delta$ rather than exact values x_{s+1}^* . The second term captures the linear interpolation error as in Lemma 4.3.

4.2. Greedy Multiscale. We use the following approach to show convergence of the greedy multiscale algorithm described in Algorithm 2.1. At each scale s , we

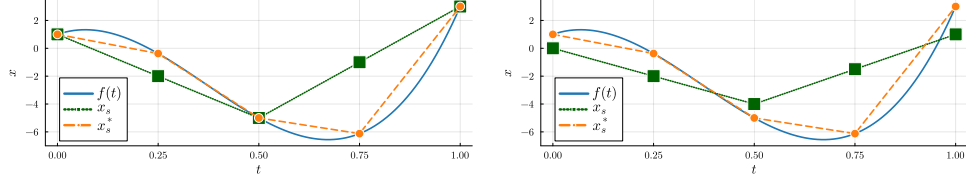


Fig. 6: Illustration of Lemma 4.3 (left) and Lemma 4.4 (right) for the function $f(t) = 72t^3 - 80t^2 + 10t + 1$. Both lemmas bound the error between the true fine-scale discretization x_s^* (orange circles) and the linear interpolation $x_s = \underline{x}_{s+1}$ (green squares) obtained from a coarser-scale discretization. The left figure shows (4.2), where $x_{s+1} = x_{s+1}^*$ is exact. The right figure shows (4.3), where $x_{s+1} = x_{s+1}^* + \delta$ contains error.

use the iterate convergence (Definition 2.5) to bound the error between our iterate $x_s^{K_s}$ and the solution x_s^* at that scale. Then we use the inexact interpolation lemma (Lemma 4.4) to bound the error between our iterate $x_s^{K_s}$ and interpolation $\underline{x}_S^{K_s}$. This interpolated iterate becomes the initialization $x_{S-1}^0 = \underline{x}_S^{K_s}$ at the next finest scale.

THEOREM 4.5 (Greedy Multiscale Error Bound). *Let q denote the rate of convergence of an algorithm applied to a loss function \tilde{L} , let L_{f^*} be the Lipschitz constant of the solution function f^* , and let S denote the coarsest scale. The greedy multiscale method in Algorithm 2.1 returns iterate $x_1^{K_1}$ at the finest scale satisfying*

$$\left\| x_1^{K_1} - x_1^* \right\|_2 \leq \sqrt{2^{S-1}} (q)^{r_s} \left\| x_S^0 - x_S^* \right\|_2 + L_{f^*} \frac{|u-\ell|}{2\sqrt{2^{S+1}}} \sum_{s=1}^{S-1} 2^s (q)^{r_s},$$

where $r_s = \sum_{t=1}^s K_t$ denotes the cumulative iteration count through scale s .

Proof. See subsection A.5. □

4.3. Lazy Multiscale. We establish convergence of the lazy multiscale algorithm using the framework from Theorem 4.5. The key modification is to freeze the interpolated values $\underline{x}_S^{K_s}$ that correspond to points from the previous iteration $x_S^{K_s}$. The algorithm updates only the newly interpolated values, denoted $x_{(s)}^k$ (see Definition 2.3).

THEOREM 4.6 (Lazy Multiscale Error Bound). *Assume the same setup as Theorem 4.5. The lazy multiscale method in Algorithm 2.1 returns iterate $x_1^{K_1}$ satisfying*

$$\left\| x_1^{K_1} - x_1^* \right\| \leq \left\| x_S^0 - x_S^* \right\| d(K_S) p(S) + \frac{1}{2} L_{f^*} |u - \ell| \sum_{s=1}^{S-1} \frac{1}{\sqrt{2^{S-s}}} d(K_s) p(s),$$

where $d(K) = (q)^K \in (0, 1)$ and $p(s) = \prod_{j=1}^{s-1} (1 + (q)^{K_j})$. When using constant iterations $K_s = K$ at each scale, this reduces to

$$\begin{aligned} \left\| x_1^{K_1} - x_1^* \right\| &\leq \left\| x_S^0 - x_S^* \right\| d(K) (d(K) + 1)^{S-1} \\ &\quad + \frac{1}{2} L_{f^*} |u - \ell| d(K) \frac{\sqrt{2^S} (d(K) + 1)^S - \sqrt{2} (d(K) + 1)}{\sqrt{2^S} (d(K) + 1) (\sqrt{2} d(K) + \sqrt{2} - 1)}. \end{aligned}$$

Proof. See subsection A.6. □

We summarize the convergence with Corollary 4.7.

COROLLARY 4.7 (Multiscale Convergence). *Suppose the number of iterations K_1 at the finest scale grows unbounded $K_1 \rightarrow \infty$. Then under the settings described by Theorems 4.5 and 4.6, both multiscale algorithms (Algorithm 2.1) converge to a solution x_1^* that solves (P_s) at the finest scale $s = 1$.*

5. Relation Between the Discretized and Continuous Problems. This section relates solutions of the discretized and continuous problems (P_s) and (P). We show that a small error $\|x_1^{K_1} - x^*\|_2$ in the fine-scale discretized problem solution implies a small error $\|\hat{f}_{x_1^{K_1}} - f^*\|_2$ for the continuous problem, where f^* solves (P) and $\hat{f}_{x_1^{K_1}}(t)$ denotes the piecewise linear function constructed from $x_1^{K_1}$ according to Definition 2.4. We assume $t \in \mathbb{R}^I$ forms a uniform grid on the interval $[\ell, u]$ with spacing $\Delta t = t[i+1] - t[i] = \frac{u-\ell}{I-1}$.

LEMMA 5.1 (Piecewise Linear Function Distance). *Let $f, g : \mathbb{R} \rightarrow \mathbb{R}$, and let $x, y \in \mathbb{R}^I$ be samples $x[i] = f(t[i])$ and $y[i] = g(t[i])$. Construct piecewise linear approximations (Definition 2.4) \hat{f} of f and \hat{g} of g . Then*

$$\|\hat{f} - \hat{g}\|_2^2 \leq \frac{2}{3} \Delta t \|x - y\|_2^2,$$

with equality holding when the end points are equal: $x[1] = y[1]$ and $x[I] = y[I]$.

Proof. See subsection A.7. □

We bound the L^2 distance between a Lipschitz function and its piecewise linear approximation.

LEMMA 5.2 (Piecewise Linear Function Approximation). *Let f be an L_f -Lipschitz function on $[\ell, u]$, and let \hat{f} denote its piecewise linear approximation (Definition 2.4) on the uniform grid $t \in \mathbb{R}^I$. Then*

$$\|\hat{f} - f\|_2^2 \leq \frac{2}{15} (u - \ell) \Delta t^2 L_f^2.$$

Proof. See subsection A.8. □

Lemma 5.2 compares favourably with existing results. De Boor [7, Ch. III, Eq. 17] establishes the bound

$$\|\hat{f} - f\|_2^2 \leq \frac{1}{16} \Delta t^4 \|f''\|_2^2,$$

which converges faster as the interval width $\Delta t \rightarrow 0$ (equivalently, $I \rightarrow \infty$), but requires $f \in C^2([\ell, u])$ with bounded second derivative. Lipschitz continuity and second-order differentiability doesn't suffice: for example, the parametrized soft-plus function $f(x) = \ln(1 + \exp(cx))/c$ is 1-Lipschitz for all $c > 0$, but has unbounded second derivative $f''(0) = c/2$ as $c \rightarrow \infty$.

De Boor showed the error vanishes for continuous functions (*not necessarily Lipschitz*), at a slower rate than Lemma 5.2 [7, Ch. III, Eq. 18]. Kunoth et al. [15, Sec. 1.5, Th. 18] generalizes the approximation error to functions in Sobolev spaces, achieving for *differentiable* Lipschitz functions a rate comparable to Lemma 5.2:

$$(5.1) \quad \|\hat{f} - f\|_2^2 \leq K \Delta t^2 \|f'\|_2^2$$

for some constant $K > 0$. We should not expect a better rate because Lipschitz functions are differentiable almost everywhere [13]. For Lipschitz functions, the derivative, where it exists, satisfies $|f'(x)| \leq L_f$, giving $\|f'\|_2^2 \leq (u - \ell) L_f^2$. Thus, Lemma 5.2 explicitly calculates the constant $K = 2/15$ in (5.1).

THEOREM 5.3 (Continuous Problem Connection). *Let $f : [\ell, u] \rightarrow \mathbb{R}$ be L_f -Lipschitz with discretization $x^* \in \mathbb{R}^I$. Let $x \in \mathbb{R}^I$, and construct the corresponding piecewise linear function \hat{f}_x (Definition 2.4). For $\epsilon > 0$, if $I > C\epsilon^{-1} + 1$ and $\|x - x^*\|_2^2 < D\epsilon$ then*

$$\|\hat{f}_x - f\|_2 < \epsilon,$$

where $C = \sqrt{\frac{8}{15}}(u - \ell)^{3/2}L_f$ and $D = \sqrt{\frac{3}{40}}(u - \ell)^{1/2}L_f$.

Proof. See subsection A.9. □

Theorem 5.3 shows that an approximate solution x to the discrete problem (P_s) constructs a piecewise linear function \hat{f}_x that approximately solves the continuous problem (P) , provided the grid is sufficiently fine. The constant C grows with the Lipschitz constant L_f , which reflects the expected behaviour that functions with greater variation require finer grids.

6. Comparison with Projected Gradient Descent. Corollary 4.7 established that two versions of the multiscale algorithm (lazy and greedy) converge to a solution of (P_s) . We now demonstrate that this convergence improves upon only solving (P_s) at the finest scale $s = 1$.

Lemma 2.6 establishes iterate convergence (Definition 2.5) for projected gradient descent. Using this, we derive expected convergence bounds for three approaches: projected gradient descent at scale $s = 1$ (Theorem 6.1), greedy multiscale descent (Theorem 6.3), and lazy multiscale descent (Theorem 6.7). We demonstrate that both multiscale variants achieve tighter error bounds with lower computational cost when the problem size is sufficiently large.

THEOREM 6.1 (Expected Projected Gradient Descent Convergence). *Consider problem (P_s) with $I = 2^S + 1$ discretization points for some $S \geq 1$, solved at the finest resolution (scale $s = 1$). Assume solutions $x_1^* \in \mathbb{R}^I$ are either normalized $\|x_1^*\|_2 = 1$ or centered $\|x_1^*\|_2 = 0$. Given initialization $x_1^0 \in \mathbb{R}^I$ with i.i.d. standard normal entries $x_1^0[i] \sim \mathcal{N}(0, 1)$, iterating projected gradient descent K times yields the expected error*

$$(6.1) \quad \mathbb{E} \|x_1^K - x_1^*\| \leq (q)^K \sqrt{2^S + 2}.$$

COROLLARY 6.2 (Expected Number of Iterations). *If we iterate projected gradient descent K times, where $K \geq (\log(1/\epsilon) + \log(2^S + 2)/2) / (-\log q)$, then the expected error is bounded as $\mathbb{E} \|x_1^K - x_1^*\|_2 \leq \epsilon$.*

Proof. See subsection A.10. □

THEOREM 6.3 (Expected Greedy Multiscale Convergence). *Assume the same setting as Theorem 6.1, but use the greedy multiscale descent method starting at scale $s = S$. Performing K_s iterations at each scale yields the expected final error*

$$(6.2) \quad \mathbb{E} \|x_1^{K_1} - x_1^*\|_2 \leq (q)^{K_1} \sqrt{2^{S+1}} \left((q)^{r_S} + \frac{L_{f^*} |u - \ell|}{2^{S+2}} \sum_{s=1}^{S-1} 2^s (q)^{r_s} \right)$$

where $r_s = \sum_{t=2}^s K_t$ with the base case $r_1 = 0$.

Proof. The result follows from Theorems 4.5 and 6.1 with the initial error bound $\mathbb{E} [\|x_S^0 - x_S^*\|] \leq (q)^0 \sqrt{2^1 + 2} = 2$ starting at the coarsest scale with $I = 3$ points. □

Determining the iteration count required to achieve a specified accuracy is less direct for multiscale methods than for projected gradient descent. Moreover, a fair

comparison requires accounting for computational cost: an iteration at coarse scale S requires fewer floating-point operations than an iteration at the finest scale $s = 1$. We therefore configure each iteration of multiscale to simultaneously achieve lower total cost than fine-scale-only optimization while obtaining a tighter expected error bound. Specifically, we require (6.2) to be smaller than (6.1). This requires costing multiscale in terms of one projected gradient descent iteration at the finest scale $s = 1$.

LEMMA 6.4 (Cost of Greedy Multiscale). *Suppose projected gradient descent with K iterations at the finest scale $s = 1$ has total cost $C_{\text{GD}} = CK$, where $C > 0$ is the cost per iteration at that scale. Assume the cost C of one projected gradient descent iteration scales polynomially $C = \Theta(I^p)$ with the problem size I for some constant $p \geq 1$. Then greedy multiscale descent with K_s iterations at scale s has total cost C_{GM} that satisfies $C_{\text{GM}} \leq C \sum_{s=1}^S K_s \left(\frac{3}{5}\right)^{s-1}$.*

With $K_s = 1$ at every scale except the finest, where $K_1 = K - 2$, $C_{\text{GM}} < C_{\text{GD}}$.

Proof. See subsection A.11. □

The assumption that iteration cost scales as $\Theta(I^p)$ for $p \geq 1$ holds for common projects and gradient computations. For example, the Euclidean projection of a vector $y \in \mathbb{R}^I$ onto the sphere \mathcal{S}^{I-1} scales linearly in I ($p = 1$). The least-squares gradient update $x \leftarrow x - A^\top(Ax - y)$ for $A \in \mathbb{R}^{I \times I}$ scales quadratically in I ($p = 2$).

The analysis in Lemma 6.4 ignores the cost of interpolation and memory allocation when changing iterate dimensions between scales. These costs become negligible as the iteration counts increase. Empirical results in Figure 3 and section 7 confirm that greedy multiscale remains cheaper in practice.

Having established conditions that ensure greedy multiscale is cheaper than projected gradient descent, we now establish conditions that ensure tighter expected error bounds.

COROLLARY 6.5 (Sufficient Conditions for Greedy Multiscale to be Better). *Assume the base algorithm has iterate convergence (Definition 2.5) with rate $q \in (0, 1/2)$. Assume the finest scale problem has $I = 2^S + 1$ points, where the number of scales S satisfies*

$$S \geq \max \left\{ 4, \log_2 \left(\frac{L_{f^*} |u - \ell|}{\sqrt{2}(q)^2 (1 - 2q)(1 - \sqrt{2}q)} \right) \right\}.$$

Then greedy multiscale with one iteration $K_s = 1$ at each scale except the finest (where $K_1 = K - 2$) simultaneously achieves lower total cost and a tighter expected final error bound than projected gradient descent with K iterations.

Proof. See subsection A.12. □

We establish analogous results for lazy multiscale.

LEMMA 6.6 (Cost of Lazy Multiscale). *Suppose the same set up as Lemma 6.4. Lazy multiscale descent with K_s iterations at scale s has a total cost C_{LM} satisfying*

$$C_{\text{LM}} \leq C \left(\sum_{s=1}^{S-1} 2^{-s} K_s + 2^{-S} 3K_S \right).$$

With $K_s = \lceil \frac{4}{5}K \rceil - 1$ iterations at each scale, $C_{\text{LM}} < C_{\text{GD}}$.

Proof. See subsection A.13 □

THEOREM 6.7 (Expected Lazy Multiscale Convergence). *Assume the same setting as Theorem 6.1, but use the lazy multiscale starting at coarsest scale S with $I = 2^S + 1$*

points at the finest scale. Performing constant $K_s = K$ iterations at each scale yields the expected final error

$$(6.3) \quad \mathbb{E} \|x_1^K - x_1^*\|_2 \leq d(K) \left(2(d(K) + 1)^{S-1} + \frac{L_{f^*}}{2} |u - \ell| \frac{\sqrt{2^S} (d(K) + 1)^S - \sqrt{2} (d(K) + 1)}{\sqrt{2^S} (d(K) + 1) (\sqrt{2} d(K) + \sqrt{2} - 1)} \right),$$

where $d(K) = (q)^K$ and the solution function f^* is L_{f^*} -Lipschitz on $[\ell, u]$.

Proof. The proof is similar to Theorem 6.3 by using Theorem 4.6. \square

We establish sufficient conditions that ensure lazy multiscale achieves both lower cost and tighter error bounds than projected gradient descent.

COROLLARY 6.8 (Sufficient Conditions for Lazy Multiscale to be Better). *Assume the base algorithm has iterate convergence (Definition 2.5) with rate $q \in (0, 1)$. Assume projected gradient decent runs for $K > 5(\log_q(\sqrt{2} - 1) - 1)/4$ iterations, and lazy multiscale runs for $K' = \lceil 4K/5 \rceil - 1$ iterations at every scale. If the finest scale has at least $I = 2^S + 1$ points where*

$$S \geq \log \left(\frac{q^{-K/5-1}}{1 + q^{K'}} \left(2 + \frac{L_{f^*} |u - \ell|}{2(\sqrt{2}(1 + q^{K'}) - 1)} \right) \right) / \log \left(\frac{\sqrt{2}}{1 + q^{K'}} \right),$$

then lazy multiscale is cheaper and achieves a tighter expected error bounds than projected gradient descent.

Proof. See subsection A.14. \square

Corollaries 6.5 and 6.8 reveal several insights. Both multiscale variants require a minimum number of scales S (equivalently a minimum sized problem I) for the multiscale optimization to outperform single scale methods. Theorem 5.3 establishes that arbitrarily small error between continuous and discretized solutions requires arbitrarily large problem size I . Both corollaries show that the required I increases with the Lipschitz constant L_{f^*} and the domain size $|u - \ell|$, consistent with Theorem 5.3. A subtle requirement is that the base algorithm cannot have iterative convergence with $q = 0$, which would enable solving the discretized problem in one iteration, and thus eliminate the benefit of multiscale.

Corollaries 6.5 and 6.8 differ in their constraints on the convergence rate q . Greedy multiscale with one iteration per scale requires convergence rate $q \in (0, 1/2)$ because interpolation error must remain smaller than the algorithmic progress at each scale. Lazy multiscale, on the other hand, allows $q \in (0, 1)$ but requires a minimum of $K' > \log_q(\sqrt{2} - 1)$ iterations at each scale to sufficiently control error accumulation. This is a mild requirement: two iterations per scale suffice for lazy multiscale to improve on the base algorithm when $0 < q < (\sqrt{2} - 1)^{1/2} \approx 0.6436$, and both algorithms require arbitrarily many iterations to drive the final error to zero.

7. Numerical Experiments and Benchmarks. We evaluate the greedy multiscale method on two density demixing problems and compare it to standard projected gradient descent. These problems seek to recover mixtures of continuous probability densities from noisy samples. We consider synthetic data in subsection 7.2 and geological survey data in subsection 7.3.

The projected-gradient multiscale and single-scale algorithms are implemented in the Julia package `BlockTensorFactorization.jl` [20]: the function `factorize`

implements projected gradient descent for the Tucker-1 decomposition problem at a single scale, and `multiscale_factorize` implements the greedy multiscale method (Algorithm 2.1). All experiments ran on an Intel Core i7-1185G7 with 32GB of RAM, without parallelization, matching the hardware used for the example experiment in subsection 2.3.

7.1. Density Demixing as Optimization. Graham et. al. [11] provides a full treatment of this formulation which we summarize here. Additional details are given in section SM3.

Given I mixtures $y_i : \mathcal{D} \subseteq \mathbb{R}^N \rightarrow \mathbb{R}_+$ of R source probability density functions $b_r : \mathcal{D} \subseteq \mathbb{R}^N \rightarrow \mathbb{R}_+$, $y_i(x) = \sum_{r \in [R]} a_{i,r} b_r(x)$, we seek to recover the sources $\{b_r\}$ and their mixing coefficients $a_{i,r}$. We assume $R < I$ and that the source densities $\{b_r\}$ are linearly independent, which ensures this is a well-posed problem.

The continuous problem formulation is

$$\min_{\{a_{i,r}\}, \{b_r\}} \frac{1}{2} \sum_{i \in [I]} \left\| \sum_{r \in [R]} a_{i,r} b_r - y_i \right\|_2^2$$

such that for all $i \in [I]$,

$$(7.1a) \quad 1 = \sum_{r \in [R]} a_{i,r}, \quad a_{i,r} \geq 0,$$

$$(7.1b) \quad 1 = \int_{\mathcal{D}} b_r(x) dx, \quad b_r(x) \geq 0 \quad \forall x \in \mathcal{D}, \forall r \in [R].$$

Discretizing yields the Tucker-1 decomposition problem (see Definition SM3.1)

$$\min \left\{ \frac{1}{2} \|B \times_1 A - Y\|_F^2 \mid A \in \Delta_R^I, B \in \Delta_{K_1 \dots K_N}^R \right\},$$

$$(7.2a) \quad \Delta_R^I = \left\{ A \in \mathbb{R}_+^{I \times R} \mid \sum_{r=1}^R A[i, r] = 1, \forall i \in [I] \right\},$$

$$(7.2b) \quad \Delta_{K_1 \dots K_N}^R = \left\{ B \in \mathbb{R}_+^{R \times K_1 \times \dots \times K_N} \mid \sum_{k_1, \dots, k_N=1}^{K_1 \dots K_N} B[r, k_1, \dots, k_N] = 1, \forall r \in [R] \right\}.$$

In the geological data example (subsection 7.3), each dimension of b_r is independent. This allows a simpler discretization, so that B becomes a third-order tensor with

$$B \in \Delta_K^{R,J} = \left\{ B \in \mathbb{R}_+^{R \times J \times K} \mid \sum_{k=1}^K B[r, j, k] = 1, \forall (r, j) \in [R] \times [J] \right\},$$

and we reinterpret $Y \in \mathbb{R}_+^{I \times J \times K}$ accordingly.

7.2. Synthetic Data. We generate three source distributions for a synthetic test. Each distribution is a 3-dimensional product of standard distributions; see section SM4 this paper’s GitHub repository [21] for details. Benchmarking the two approaches across 20 samples yields the following for the single-scale `factorize` function:

Range (min...max):	1.305 s...3.487 s	GC (min...max):	15.07%
Time (median):	2.412 s	GC (median):	27.67%
Time (mean \pm σ):	2.418 s \pm 628.420 ms	GC (mean \pm σ):	25.08%
Memory estimate:	1.46 GiB, allocs estimate:	2189884.	

and for the factorization at multiple scales with the `multiscale_factorize` function:

Range (min...max):	231.299 ms...1.583 s	GC (min...max):	8.10%
Time (median):	334.698 ms	GC (median):	11.61%
Time (mean \pm σ):	455.869 ms \pm 313.358 ms	GC (mean \pm σ):	23.90%
Memory estimate:	366.81 MiB, allocs estimate:		569530.

The function `multiscale_factorize` runs roughly seven times faster and uses about one-fourth of the memory. This comparison includes overhead such as interpolating the tensor and repeatedly calling the internal `factorize` function, which represents approximately 4% of the total time. The specific numbers are less important than the qualitative comparison: both algorithms could be optimized and benchmarked on state-of-the-art hardware, but this basic implementation demonstrates that multiscale methods can accelerate single-scaled algorithms.

In these `multiscale_factorize` benchmarks, rather than performing one iteration at each scale coarser than the finest scale, we advance to the next scale once sufficient progress has been made; see section SM4 for details. This differs from our analysis in Corollary 6.5, which suggests using exactly $K_s = 1$ at coarse scales. However, running additional iterations at coarser scales often reduces the total number of iterations required at the finest scale.

Figure 7 (left) shows median runtime as a function of the number of fixed coarse iterations K_s in multiscale for $s = S, S-1, \dots, 2$, where we run iterations at the finest scale until the objective falls below 10^{-6} . This figure demonstrates that performing more than one iteration at coarser scales improves multiscale performance, but only to a point: in Figure 7 (left), more than 12 iterations at each coarse scale wastes time. Figure 7 (right) illustrates this by showing the number of fine-scale iterations K_1 needed to converge to a minimum value. Our implementation of `multiscale_factorize` [20] addresses this by allowing multiple iterations at coarser scales and advancing to the next scale when other criteria are met, such as small gradients or objective values.

Both plots in Figure 7 show that multiscale with exactly $K_s = 1$ iterations at coarse scales $s = S, S-1, \dots, 2$ performs slightly worse than single-scale optimization. We attribute this to interpolation and to overhead costs in the multiscale approach. The problem size of $2^6 + 1 = 65$ points along each continuous dimension may be too small to see immediate benefit from multiscale when only one iteration is performed at each scale; larger problems may needed to realize the advantage illustrated by Figure 1. However, flexible criteria to advance between scales may make multiscale competitive even for smaller problems as shown in the benchmark tests.

7.3. Real Geological Data. We use the same sedimentary data and Tucker-1 model described in Graham et. al. [11] to factorize a tensor containing mixtures of estimated densities. Subsection SM4.1 provides the details, and the full code appears in `distribution_unmixing_geology.jl` in this paper’s GitHub repository [21]. For `factorize` and `multiscale_factorize`, we obtain the respective benchmarks:

Range (min...max):	174.316 ms...593.727 ms	GC (min...max):	19.75%
Time (median):	416.816 ms	GC (median):	19.91%
Time (mean \pm σ):	389.401 ms \pm 108.955 ms	GC (mean \pm σ):	19.90%
Memory estimate:	361.43 MiB, allocs estimate:		139855.

Range (min...max):	78.320 ms...153.810 ms	GC (min...max):	0.00%
Time (median):	91.376 ms	GC (median):	0.00%
Time (mean \pm σ):	95.542 ms \pm 19.154 ms	GC (mean \pm σ):	11.24%
Memory estimate:	105.80 MiB, allocs estimate:		1444133.

By every metric, the multiscale approach is faster and uses less memory than the

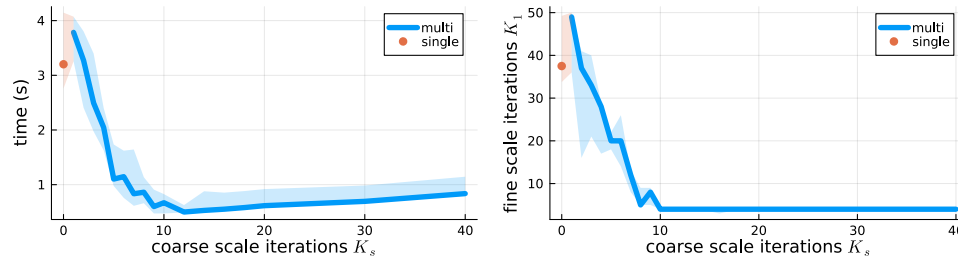


Fig. 7: (Left) Median time until convergence at the finest scale $s = 1$ as a function of number of fixed iterations K_s at coarser scales $s = S, S - 1, \dots, 2$. (Right) Median number of iterations K_1 at the finest scale $s = 1$. Shaded ribbon shows the bottom and top quartile times (left) and iterations (right).

standard single-scale factorization. Comparing median time and memory estimates, the multiscale method runs roughly four times faster with about a third of the memory.

8. Conclusion. We developed a multiscale approach for optimizing Lipschitz continuous functions by solving discretized problems at progressively finer scales. Our convergence analysis establishes that both greedy and lazy variants achieve the finest-scale solution through per-scale descent combined with controlled interpolation error. The framework extends to linear and norm constraints and tensor-valued functions.

The explicit error bounds derived quantify the tradeoff between discretization granularity and solution accuracy, and prove that multiscale outperforms direct fine-scale optimization when the problem size and Lipschitz constant are sufficiently large.

Several directions merit further investigation. Our analysis assumes a fixed number of base algorithm iterations at each scale. However, an adaptive iteration count that responds to convergence progress could improve efficiency. With regard to the discretization, the dyadic scheme might be replaced by adaptive grid refinement based on local Lipschitz estimates. Second-order base algorithms present another avenue, though their cost would be better characterized in terms of linear system solves rather than gradient evaluations. Finally, interpreting the pointwise discretization as a discrete wavelet transform suggests generalizations to other wavelet expansions.

REFERENCES

- [1] B. ADCOCK, M. J. COLBROOK, AND M. NEYRA-NESTERENKO, *Restarts Subject to Approximate Sharpness: A Parameter-Free and Optimal Scheme For First-Order Methods*, Found. Comput. Math., (2025).
- [2] A. ANG, H. DE STERCK, AND S. VAVASIS, *MGProx: A Nonsmooth Multigrid Proximal Gradient Method with Adaptive Restriction for Strongly Convex Optimization*, SIOPT, 34 (2024).
- [3] J. J. BENEDETTO AND M. W. FRAZIER, *Wavelets: Mathematics and Applications*, CRC Press, Boca Raton, 1st ed., 1993.
- [4] S. CHAKRABORTY, *Generating discrete analogues of continuous probability distributions-A survey of methods and constructions*, J. Stat. Distributions Appl., 2 (2015).
- [5] Y.-C. CHEN, *A tutorial on kernel density estimation and recent advances*, Biostat. & Epidemiol., 1 (2017).
- [6] T. CHUNA, N. BARNFIELD, T. DORNHEIM, M. P. FRIEDLANDER, AND T. HOHEISEL, *Dual formulation of the maximum entropy method applied to analytic continuation of quantum Monte Carlo data*, 2025.
- [7] C. DE BOOR, *A practical guide to splines*, no. v. 27 in Applied mathematical sciences, Springer, New York, rev. ed., 2001.

- [8] I. DHILLON, P. RAVIKUMAR, AND A. TEWARI, *Nearest Neighbor based Greedy Coordinate Descent*, in NeurIPS, vol. 24, Curran Associates, Inc., 2011.
- [9] I. M. GELFAND AND S. V. FOMIN, *Calculus of variations*, Dover Books, Mineola, N.Y., 2000.
- [10] N. GILLIS AND F. GLINEUR, *A multilevel approach for nonnegative matrix factorization*, J. Comput. Appl. Math., 236 (2012).
- [11] N. GRAHAM, N. RICHARDSON, M. P. FRIEDLANDER, AND J. SAYLOR, *Tracing Sedimentary Origins in Multivariate Geochronology via Constrained Tensor Factorization*, Math. Geosci., (2025).
- [12] K. GURNEY, *An Introduction to Neural Networks*, CRC Press, London, 2018.
- [13] J. HEINONEN, *Lectures On Lipschitz Analysis*. 2004.
- [14] R. KONDOR, N. TENEVA, AND V. GARG, *Multiresolution Matrix Factorization*, in Proceedings of the 31st ICML, PMLR, 2014.
- [15] A. KUNOTH, T. LYCHE, G. SANGALLI, AND S. SERRA-CAPIZZANO, *Splines and PDEs: From Approximation Theory to Numerical Linear Algebra*, vol. 2219 of Lecture Notes in Math., Springer, 2018.
- [16] I. LOSCHILOV AND F. HUTTER, *SGDR: Stochastic Gradient Descent with Warm Restarts*, 2017.
- [17] Y. NESTEROV, *Efficiency of Coordinate Descent Methods on Huge-Scale Optimization Problems*, SIOPT, 22 (2012).
- [18] Y. NESTEROV, *Smooth Convex Optimization*, in Lectures on Convex Optimization, Y. Nesterov, ed., SOIA, Springer International Publishing, Cham, 2018.
- [19] S. RAMÍREZ-GALLEGO, S. GARCÍA, H. MOURIÑO-TALÍN, D. MARTÍNEZ-REGO, V. BOLÓN-CANEDO, A. ALONSO-BETANZOS, J. M. BENÍTEZ, AND F. HERRERA, *Data discretization: taxonomy and big data challenge*, WIREs Data Min. Knowl. Discov., 6 (2016).
- [20] N. RICHARDSON, N. MARUSENKO, AND M. P. FRIEDLANDER, *BlockTensorFactorization.jl v0.4.0*. <https://github.com/MPF-Optimization-Laboratory/BlockTensorFactorization.jl>, 2025.
- [21] ———, *richardson-multiscale-2025*. <https://github.com/MPF-Optimization-Laboratory/richardson-multiscale-2025>, 2025.
- [22] H. J. STETTER, *Analysis of Discretization Methods for Ordinary Differential Equations*, no. 23 in Springer Tracts in Natural Philosophy, Springer, Berlin Heidelberg, 1973.
- [23] V. STRASSEN, *Gaussian elimination is not optimal*, Numer. Math., 13 (1969).
- [24] L. N. TREFETHEN, *Approximation theory and approximation practice*, no. 164 in Other titles in applied mathematics, SIAM, Philadelphia, extended ed., 2019.
- [25] U. TROTTEMBERG, C. W. OOSTERLEE, AND A. SCHULLER, *Multigrid Methods*, AP, 2001.
- [26] R. VERSHYNIN, *High-Dimensional Probability*, Cambridge Series in Statistical and Probabilistic Mathematics, Cambridge University Press, 2018.
- [27] Y. XU AND W. YIN, *A Block Coordinate Descent Method for Regularized Multiconvex Optimization with Applications to Nonnegative Tensor Factorization and Completion*, SIIMS, 6 (2013).
- [28] Y. YAN, K. WANG, AND P. RIGOLLET, *Learning Gaussian Mixtures Using the Wasserstein-Fisher-Rao Gradient Flow*, 2023.

Appendix A. Proofs.

A.1. Proof of Proposition 3.3 (Single Linear Constraint Scaling). For an even number of points I , we have

$$\begin{aligned} |2 \langle \bar{a}, \bar{x} \rangle - b| &= \left| 2 \sum_{i \text{ odd}} a[i]x[i] - \sum_{i=1}^I a[i]x[i] \right| = \left| \sum_{i \text{ odd}} a[i]x[i] - \sum_{i \text{ even}} a[i]x[i] \right| \\ &\leq \sum_{i \text{ odd}} |a[i]x[i] - a[i+1]x[i+1]| \leq \sum_{i \text{ odd}} L_{fg} \Delta t |i - (i+1)| = \frac{I}{2} L_{fg} \frac{u-l}{I-1}. \end{aligned}$$

The second inequality follows from Corollary 3.2 in combination with the product $a[i]x[i] = f(t[i])g(t[i])$ being Lipschitz with constant $L_{fg} = (L_f \|g\|_\infty + L_g \|f\|_\infty)$ (see Lemma SM1.4). Dividing by 2 proves the first statement.

For odd I , we have

$$\begin{aligned} |2 \langle \bar{a}, \bar{x} \rangle - (1 + \frac{1}{I})b| &= \left| \sum_{i \text{ odd}} a[i]x[i] - \sum_{i \text{ even}} a[i]x[i] - \frac{1}{I}b \right| \\ &= \left| \sum_{j=1}^{(I-1)/2} a[2j-1]x[2j-1] + a[I]x[I] - \sum_{j=1}^{(I-1)/2} a[2j]x[2j] - \frac{1}{I}b \right| \\ &\leq \sum_{j=1}^{(I-1)/2} |a[2j-1]x[2j-1] - a[2j]x[2j]| + \frac{1}{I} |Ia[I]x[I] - b| \\ &= \sum_{j=1}^{(I-1)/2} |a[2j-1]x[2j-1] - a[2j]x[2j]| + \frac{1}{I} \sum_{i=1}^I |a[i]x[i] - a[i]x[i]| \end{aligned}$$

The first sum is bounded by $\frac{I-1}{2} L_{fg} \frac{u-l}{I-1} = L_{fg} \frac{u-l}{2}$ in a similar manner to the even I case. The second term is bounded by $\frac{1}{I} \sum_{i=1}^I L_{fg} \Delta t |I-i| = \frac{1}{I} L_{fg} \frac{u-l}{I-1} \frac{I(I-1)}{2} = L_{fg} \frac{u-l}{2}$. Adding these terms together gives us the bound $|2 \langle \bar{a}, \bar{x} \rangle - \frac{I+1}{I} b| \leq L_{fg}(u-l)$. Dividing by 2 completes the proof.

In the following proofs, we take the unlabeled norm $\|\cdot\| = \|\cdot\|_2$ to be the 2-norm.

A.2. Proof of Lemma 4.1 (Lipschitz Function Interpolation). Let $f : \mathbb{R}^n \rightarrow \mathbb{R}$ be L_f -Lipschitz, $a, b \in \mathbb{R}^n$, and $\lambda = \lambda_1$, $1 - \lambda = \lambda_2$ for $\lambda \in [0, 1]$. Our goal is to bound $|((1 - \lambda)f(a) + \lambda f(b)) - f((1 - \lambda)a + \lambda b)|$. We achieve the tightest bound by separating $f((1 - \lambda)a + \lambda b) = (1 - \lambda)f((1 - \lambda)a + \lambda b) + \lambda f((1 - \lambda)a + \lambda b)$ and using triangle inequality to get

$$\begin{aligned} & |((1 - \lambda)f(a) + \lambda f(b)) - f((1 - \lambda)a + \lambda b)| \\ & \leq |(1 - \lambda)f(a) - (1 - \lambda)f((1 - \lambda)a + \lambda b)| + |\lambda f(b) - \lambda f((1 - \lambda)a + \lambda b)| \\ & \leq (1 - \lambda)L_f \|a - ((1 - \lambda)a + \lambda b)\|_2 + \lambda L_f \|b - ((1 - \lambda)a + \lambda b)\|_2 \\ & = 2\lambda(1 - \lambda)L_f \|a - b\|_2. \end{aligned}$$

A.3. Proof of Lemma 4.3 (Exact Interpolation). Using Lemma 4.1 with $\lambda = 1/2$, we have for even j ,

$$\begin{aligned} |x_s[j] - x_s^*[j]| &= \left| \frac{1}{2}(x_{s+1} \left[\frac{j}{2} \right] + x_{s+1} \left[\frac{j}{2} + 1 \right]) - f(t_s[j]) \right| \\ &= \left| \frac{1}{2}(f(t_{s+1} \left[\frac{j}{2} \right]) + f(t_{s+1} \left[\frac{j}{2} + 1 \right])) - f\left(\frac{1}{2}(t_{s+1} \left[\frac{j}{2} \right] + t_{s+1} \left[\frac{j}{2} + 1 \right])\right) \right| \\ &\leq \frac{L_f}{2} |t_{s+1} \left[\frac{j}{2} \right] - t_{s+1} \left[\frac{j}{2} + 1 \right]| = \frac{L_f}{2(I-1)} |\alpha - \beta|. \end{aligned}$$

For odd j , the interpolated values match the function exactly

$$x_s[j] = \underline{x}_{s+1}[j] = x_{s+1} \left[\frac{j+1}{2} \right] = x_{s+1}^* \left[\frac{j+1}{2} \right] = f(t_{s+1} \left[\frac{j+1}{2} \right]) = f(t_s[j]) = x_s^*[j].$$

Summing over all j , we bound the squared error

$$\begin{aligned} \|x_s - x_s^*\|_2^2 &= \sum_{j=1}^J |x_s[j] - x_s^*[j]|^2 = \sum_{j \text{ even}} |x_s[j] - x_s^*[j]|^2 \\ &\leq \sum_{j \text{ even}} \frac{L_f^2}{4(I-1)^2} |\alpha - \beta|^2 \leq (I-1) \frac{L_f^2}{4(I-1)^2} |\alpha - \beta|^2 = \frac{L_f^2}{4(I-1)} |\alpha - \beta|^2. \end{aligned}$$

Taking square roots completes the proof.

A.4. Proof of Lemma 4.4 (Inexact Interpolation). Let the inexact values be $x_{s+1}[i] = x_{s+1}^*[i] + \delta[i]$, and interpolate to get $x_s = \underline{x}_{s+1}$:

$$\begin{aligned} & \underline{x}_{s+1}[j] \\ &= \begin{cases} x_{s+1} \left[\frac{j+1}{2} \right] &= x_{s+1}^* \left[\frac{j+1}{2} \right] + \delta \left[\frac{j+1}{2} \right], & j \text{ odd,} \\ \frac{1}{2}(x_{s+1} \left[\frac{j}{2} \right] + x_{s+1} \left[\frac{j}{2} + 1 \right]) &= \frac{1}{2}(x_{s+1}^* \left[\frac{j}{2} \right] + x_{s+1}^* \left[\frac{j}{2} + 1 \right] + \delta \left[\frac{j}{2} \right] + \delta \left[\frac{j}{2} + 1 \right]), & j \text{ even.} \end{cases} \end{aligned}$$

Let $e = \underline{x}_{s+1}[j] - x_s^*[j]$. Note \underline{x}_{s+1} is the interpolated vector of x_{s+1}^* where $x_{s+1}^*[i] = f(t_{s+1}[i])$, and is possibly different from the exact discretization $x_s^*[j] = f(t_s[j])$. Of course the entries $\underline{x}_{s+1}^*[j] = x_s^*[j]$ for odd j . We can now bound $\|e\|$ in terms of δ .

$$\|e\|^2 = \sum_{j \text{ odd}} \left| \delta \left[\frac{j+1}{2} \right] \right|^2 + \sum_{j \text{ even}} \left| \frac{1}{2} (\delta \left[\frac{j}{2} \right] + \delta \left[\frac{j}{2} + 1 \right]) \right|^2 = \|\delta\|^2 + \frac{1}{4} \sum_{i=1}^{I-1} (\delta[i] + \delta[i+1])^2$$

$$\begin{aligned}
&\leq \|\delta\|^2 + \frac{1}{4} \left(\sum_{i=1}^I \delta[i]^2 + \sum_{i=0}^{I-1} \delta[i+1]^2 + 2 \sum_{i=1}^{I-1} \delta[i]\delta[i+1] \right) \\
&\leq \frac{3}{2} \|\delta\|^2 + \frac{1}{2} \left(\sum_{i=1}^I \delta[i]^2 \right)^{1/2} \left(\sum_{i=0}^{I-1} \delta[i+1]^2 \right)^{1/2} \quad (\text{Cauchy-Schwarz, add } \delta[I], \delta[0]) \\
&= \frac{3}{2} \|\delta\|^2 + \frac{1}{2} \|\delta\| \|\delta\| = 2 \|\delta\|^2
\end{aligned}$$

Taking square roots and substituting gives us $\|\underline{x}_{s+1} - \underline{x}_{s+1}^*\| \leq \sqrt{2} \|x_{s+1} - x_{s+1}^*\|$.

We use triangle inequality and Lemma 4.3 to bound the difference between the interpolated approximate values $x_s = \underline{x}_{s+1}$ and the true values x_s^* :

$$\begin{aligned}
\|x_s - x_s^*\|_2 &\leq \|x_s - \underline{x}_{s+1}\|_2 + \|\underline{x}_{s+1} - x_s^*\|_2 = \|\underline{x}_{s+1} - \underline{x}_{s+1}^*\|_2 + \|\underline{x}_{s+1}^* - x_s^*\|_2 \\
&\leq \sqrt{2} \|x_{s+1} - x_{s+1}^*\|_2 + \frac{L_f}{2\sqrt{I-1}} |u - \ell|.
\end{aligned}$$

In the following proofs, we take the unlabeled norm $\|\cdot\| = \|\cdot\|_2$ to be the 2-norm.

A.5. Proof of Theorem 4.5 (Greedy Multiscale Error Bound). Using Definition 2.5, $\|x_s^{K_s} - x_s^*\| = (q)^{K_s} \|x_s^0 - x_s^*\|$ so by Lemma 4.4 we have

$$\|x_{s-1}^0 - x_{s-1}^*\| = \|\underline{x}_s^{K_s} - x_{s-1}^*\| \leq \sqrt{2}(q)^{K_s} \|x_s^0 - x_s^*\| + \frac{L|u-\ell|}{2\sqrt{2^{s-1}}}$$

Substituting $s \mapsto s+1$ and letting $e_s = \|x_s^0 - x_s^*\|$ and $C = \frac{L_f^* |u-\ell|}{2\sqrt{2^{s+1}}}$ gives us

$$e_s \leq \sqrt{2}(q)^{K_{s+1}} e_{s+1} + \sqrt{2^{s+1}} C.$$

Applying projected gradient descent on the finest scale and using this inequality recursively for $s = 1, \dots, S-1$ gives us the desired result, where $r_s = \sum_{t=1}^s K_t$,

$$\|x_1^{K_1} - x_1^*\| \leq (q)^{K-1} e_1 \leq \sqrt{2^{S-1}} (q)^{r_S} e_S + C \sum_{s=1}^{S-1} 2^s (q)^{r_s}.$$

A.6. Proof of Theorem 4.6 (Lazy Multiscale Error Bound). We first require the following lemma.

LEMMA A.1 (Inexact Lazy Interpolation). *Let $e = x - x^*$ be the error between x and the solution values $x^*[i] = f^*(t[i])$, and let $e_{(s)}$ be the error in the newly added points at the scale s (see Definition 2.3). In the lazy multiscale setting for an L_{f^*} -Lipchitz function f^* on $[\ell, u]$, we have the interpolated error bound at scale s ,*

$$\|e_{(s)}\| \leq \frac{L_{f^*} |u-\ell|}{2\sqrt{2^{s-s}}} + \|e_{s+1}\|.$$

Proof. The proof is similar to Lemma 4.4 for greedy multiscale and differs by a factor of $\sqrt{2}$ on the error term $\|e_{s+1}\|$. This is shown by modifying subsection A.4 to exclude odd indexes since we only look at the error for the newly interpolated points. \square

Using Lemma A.1 with the convergence equation (Definition 2.5) gives us

$$\|e_{(s)}^{K_s}\| \leq (q)^{K_s} \left(\frac{L_{f^*} |u-\ell|}{2\sqrt{2^{S-s}}} + \|e_{s+1}^{K_{s+1}}\| \right).$$

Using $\|e_s^{K_s}\|^2 = \|e_{(s)}^{K_s}\|^2 + \|e_{s+1}^{K_{s+1}}\|^2$, we have the recursion relation

$$\|e_s^{K_s}\|^2 \leq (q)^{2K_s} \left(\frac{C}{\sqrt{2^{S-s}}} + \|e_{s+1}^{K_{s+1}}\| \right)^2 + \|e_{s+1}^{K_{s+1}}\|^2$$

where $C = \frac{L_{f^*}}{2} |u - \ell|$. We can remove the squares because, for $a, b, c \geq 0$, having $a^2 \leq b^2 + c^2 \leq b^2 + 2bc + c^2 = (b + c)^2$ implies $a \leq b + c$. So we have a looser bound,

$$\|e_s^{K_s}\| \leq (q)^{K_s} \left(\frac{C}{\sqrt{2^{S-s}}} + \|e_{s+1}^{K_{s+1}}\| \right) + \|e_{s+1}^{K_{s+1}}\| = (1 + (q)^{K_s}) \|e_{s+1}^{K_{s+1}}\| + \frac{C(q)^{K_s}}{\sqrt{2^{S-s}}}.$$

Applying this bound recursively for every $s = 1, \dots, S-1$ gives us the general formula

$$\|e_1^{K_1}\| \leq \|e_S^{K_S}\| \prod_{s=1}^{S-1} (1 + (q)^{K_s}) + C \sum_{s=1}^{S-1} \frac{1}{\sqrt{2^{S-s}}} (q)^{K_s} \prod_{j=1}^{s-1} (1 + (q)^{K_j}).$$

Performing gradient descent on the coarsest scale lets us substitute $\|e_S^{K_S}\| \leq \|e_S^0\| (q)^{K_S}$ giving us the first upper bound for any plan of iterations K_s . If we now assume each scale uses the same number of iterations $K_s = K$, $\prod_{j=1}^{s-1} (1 + (q)^K) = (1 + (q)^K)^{s-1}$. Computing the resulting geometric sum gives the final upper bound in the theorem.

A.7. Proof of Lemma 5.1 (Piecewise Linear Function Distance).

In the following, we use the substitution $s = m_i(t - t_1) + b_i$ so that $ds = m_i dt$ where $m_i = (f(t_{i+1}) - f(t_i) - g(t_{i+1}) + g(t_i)) / \Delta t$ and $b_i = f(t_i) - g(t_i)$. We evaluate

$$\begin{aligned} \|\hat{f}_x - \hat{g}_y\|_2^2 &= \int_{t_1}^{t_I} (\hat{f}_x(t) - \hat{g}_y(t))^2 dt \\ &= \sum_{i=1}^{I-1} \int_{t_i}^{t_{i+1}} \left(\left(\frac{f(t_{i+1}) - f(t_i)}{\Delta t} - \frac{g(t_{i+1}) - g(t_i)}{\Delta t} \right) (t - t_i) + (f(t_i) - g(t_i)) \right)^2 dt \\ &= \sum_{i=1}^{I-1} \int_{t_i}^{t_{i+1}} (m_i(t - t_i) + b_i)^2 dt = \sum_{i=1}^{I-1} \frac{1}{m_i} \int_{b_i}^{m_i \Delta t + b_i} s^2 ds \\ &= \sum_{i=1}^{I-1} \frac{1}{m_i} \frac{1}{3} ((m_i \Delta t + b_i)^3 - b_i^3) = \sum_{i=1}^{I-1} \frac{\Delta t}{3} ((m_i \Delta t + b_i)^2 + b_i^2) \\ &= \frac{\Delta t}{3} \sum_{i=1}^{I-1} ((f(t_{i+1}) - g(t_{i+1}))^2 + (f(t_i) - g(t_i))^2) \\ &= \frac{\Delta t}{3} \left(2 \sum_{i=1}^I (f(t_i) - g(t_i))^2 - (f(t_1) - g(t_1))^2 - (f(t_I) - g(t_I))^2 \right) \\ &= \frac{\Delta t}{3} \left(2 \|x - y\|_2^2 - (x[1] - y[1])^2 - (x[I] - y[I])^2 \right) \leq \frac{2\Delta t}{3} \|x - y\|_2^2. \end{aligned}$$

A.8. Proof of Lemma 5.2 (Piecewise Linear Function Approximation).

By Lemma 4.1 with substitutions $a \mapsto t_{i+1}$, $b \mapsto t_i$, and $t \mapsto (t - t_i) / \Delta t$ where $\Delta t = t_{i+1} - t_i$ we have $\frac{t-t_i}{\Delta t} t_{i+1} + (1 - \frac{t-t_i}{\Delta t}) t_i = t$ and

$$\begin{aligned} & \left| \frac{t-t_i}{\Delta t} f(t_{i+1}) + \left(1 - \frac{t-t_i}{\Delta t}\right) f(t_i) - f\left(\frac{t-t_i}{\Delta t} t_{i+1} + \left(1 - \frac{t-t_i}{\Delta t}\right) t_i\right) \right| \\ & \leq 2L_f \frac{t-t_i}{\Delta t} \left(1 - \frac{t-t_i}{\Delta t}\right) |t_{i+1} - t_i| \\ \left| \frac{f(t_{i+1}) - f(t_i)}{\Delta t} (t - t_i) + f(t_i) - f(t) \right| & \leq \frac{L_f}{\Delta t} (t - t_i) (t_{i+1} - t) \\ |\hat{f}(t) - f(t)| & \leq \frac{L_f}{\Delta t} (t - t_i) (t_{i+1} - t). \end{aligned}$$

We can then bound the error, using an integration substitution of $s = t - t_i$,

$$\begin{aligned} \|\hat{f} - f\|_2^2 &= \int_{t_1}^{t_I} (\hat{f}(t) - f(t))^2 dt = \sum_{i=1}^{I-1} \int_{t_i}^{t_{i+1}} (\hat{f}(t) - f(t))^2 dt \\ &\leq \sum_{i=1}^{I-1} \int_{t_i}^{t_{i+1}} \left(\frac{2L_f}{\Delta t} (t - t_i) (t_{i+1} - t) \right)^2 dt \\ &= \frac{4L_f^2}{\Delta t^2} \sum_{i=1}^{I-1} \int_{t_i}^{t_{i+1}} (t - t_i)^2 (t_{i+1} - t)^2 dt = \frac{4L_f^2}{\Delta t^2} \sum_{i=1}^{I-1} \int_0^{\Delta t} s^2 (\Delta t - s)^2 ds \\ &= \frac{4L_f^2}{\Delta t^2} (I-1) \left(\frac{1}{3} \Delta t^2 \Delta t^3 - \frac{1}{4} 2\Delta t \Delta t^4 + \frac{1}{5} \Delta t^5 \right) = \frac{2}{15} L_f^2 \Delta t^2 (t_I - t_1). \end{aligned}$$

A.9. Proof of Theorem 5.3 (Continuous Problem Connection). Let $\epsilon > 0$, $I > \sqrt{8/15}(u - \ell)^{3/2}L\epsilon^{-1} + 1$, and $\|x - x^*\|_2^2 < \sqrt{3/40}(u - \ell)^{1/2}L\epsilon$. This means $(I - 1)^{-1} < (\epsilon\sqrt{15})/(\sqrt{8}L(u - \ell)^{3/2})$. We use triangle inequality with the piecewise linear approximation $\hat{f}_{x^*} = \hat{f}$ of f where $x^*[i] = f(t[i])$ is the true discretization of f . This gives us $\|\hat{f}_x - f\|_2 \leq \|\hat{f}_x - \hat{f}_{x^*}\|_2 + \|\hat{f}_{x^*} - f\|_2 = \|\hat{f}_x - \hat{f}_{x^*}\|_2 + \|\hat{f} - f\|_2$. By Lemma 5.1 and our bounds on $(I - 1)^{-1}$ and $\|x - x^*\|_2^2$, we bound the first term:

$$\|\hat{f}_x - \hat{f}_{x^*}\|_2^2 \leq \frac{2}{3}\Delta t \|x - x^*\|_2^2 < \frac{2}{3}\frac{u-\ell}{I-1} \left(L\epsilon\sqrt{\frac{3(u-\ell)}{40}} \right)^2 < \frac{\epsilon^2}{4}.$$

By Lemma 5.2 and our bound on $(I - 1)^{-1}$, we bound the second term:

$$\|\hat{f} - f\|_2^2 \leq \frac{2}{15}(u - \ell)L^2\Delta t^2 = \frac{2}{15}(u - \ell)L^2 \left(\frac{u-\ell}{I-1} \right)^2 < \frac{\epsilon^2}{4}.$$

Taking square roots and adding these two bounds gives us our desired result.

REMARK 2. *The statement we proved has a clean final implication, but complicates the assumptions on I and $x - x^*$. The statement can be rewritten by substituting $\epsilon \mapsto (u - \ell)\epsilon$ to show that for all $\epsilon > 0$,*

$$I > \sqrt{\frac{8}{15}}(u - \ell)L\epsilon^{-1} + 1 \text{ and } \|x - x^*\|_2^2 < \sqrt{\frac{3}{40}}(u - \ell)L\epsilon \implies \left\| \frac{\hat{f}_x - f}{u - \ell} \right\|_2 < \epsilon.$$

Rewritten, it is clearer that what matters is the effective Lipschitz constant $(u - \ell)L$, and not L and $(u - \ell)$ separately, and the right side is now expressed in terms of the average error.

A.10. Proof of Theorem 6.1 (Expected Projected Gradient Descent Convergence). Case 1: $\|x_1^*\|_2 = 1$.

Without loss of generality, assume (by symmetry) the solution x_1^* is such that $x_1^*[I] = 1$ and $x_1^*[i] = 0$ (fix a point on the sphere aligned with the I th axis) so that $x_1^* = e_I$, the unit vector $e_I = (0, \dots, 0, 1)$. Let entries of our initialization be standard Gaussian $x_1^0[i] = g[i] \sim \mathcal{N}(0, 1)$. We have

$$\begin{aligned} \mathbb{E}_{g[i] \sim \mathcal{N}} \|x_1^0 - x_1^*\|_2^2 &= \mathbb{E}_{g[i] \sim \mathcal{N}} \|g - e_I\|_2^2 = \mathbb{E}_{g[i] \sim \mathcal{N}} \left[\sum_{i=1}^{I-1} (g[i] - 0)^2 + (g[I] - 1)^2 \right] \\ &= \sum_{i=1}^{I-1} \mathbb{E}_{g[i] \sim \mathcal{N}} [g[i]^2] + \mathbb{E}_{g[I] \sim \mathcal{N}} [(g[I] - 1)^2] = (I - 1) + ((1) - 2(0) + 1) = I + 1. \end{aligned}$$

With Gaussian concentration, we can take the square root of both sides [26].

Case 2: $\|x_1^*\|_2 = 0$.

Assume the solution is centred so that $x_1^* = 0 \in \mathbb{R}^I$. Here, we have the well-known result $\mathbb{E} [\|x_1^0 - x_1^*\|] = \mathbb{E} [\|g - 0\|] = \sqrt{I}$ (see [26]).

In either case, our initial error for a scaled or centred problem goes like $\sim \sqrt{I}$. Since the number of points we have is I is one plus a power of two $I = 2^S + 1$, we expect (that is, with high probability) the convergence $\|x_1^K - x_1^*\| \leq (q)^K \sqrt{2^S + 2}$.

To ensure $\|x_1^K - x_1^*\| \leq \epsilon$ in expectation and prove Corollary 6.2, we need

$$(q)^K \sqrt{2^S + 2} \leq \epsilon \iff \left(\frac{1}{2} \log(2^S + 2) + \log(1/\epsilon) \right) / (-\log q) \leq K.$$

A.11. Proof of Lemma 6.4 (Cost of Greedy Multiscale). The total cost of regular projected gradient descent is $C_{\text{GD}} = CK$, and the cost for greedy multiscale is $C_{\text{GM}} = \sum_{s=1}^S C_s K_s$. In the case of greedy multiscale, one iteration at the finest scale

$s = 1$ costs the same for regular projected gradient descent and multiscale $C = C_1$. Assume $C_s = DI^p = D(2^{S-s+1} + 1)^p$ for some constant $D > 0$, power $p \geq 1$, and coarsest scale S , where there are $2^S + 1$ points at the finest scale $s = 1$. We wish to lower bound the ratio

$$\frac{C_s}{C_{s+1}} = \frac{D(2^{S-s+1} + 1)^p}{D(2^{S-(s+1)+1} + 1)^p} = \left(\frac{2^{S-s+1} + 1}{2^{S-s+1}} \right)^p$$

for $1 \leq s \leq S - 1$. Letting $x = S - s$, the function $g(x) = \frac{2^{x+1} + 1}{2^{x+1}}$ is increasing so it is minimized at $x = 1$ on $1 \leq x = S - s \leq S - 1$. This means $g(x) \geq g(1) = 5/3$ and, since $p \geq 1$,

$$\frac{C_s}{C_{s+1}} \geq \left(\frac{5}{3}\right)^p \geq \frac{5}{3} \implies C_1 \geq \frac{5}{3}C_2 \geq \left(\frac{5}{3}\right)^2 C_3 \geq \dots \geq \left(\frac{5}{3}\right)^{S-1} C_S.$$

Multiplying through by $(3/5)^{S-1}$ and noting $C = C_1$ gives us our final inequality and completes the proof with $C_{\text{GM}} = \sum_{s=1}^S C_s K_s \leq C_1 \sum_{s=1}^S \left(\frac{3}{5}\right)^{s-1} K_s$.

To show this is less than C_{GD} with our plan of one iteration $K_s = 1$ at all scales except the finest $K_1 = K - 2$, observe,

$$C_{\text{GM}} = C(K - 2) + C \sum_{s=2}^S \left(\frac{3}{5}\right)^{s-1} = C(K - 2) + C \frac{3/5 - (3/5)^S}{1 - (3/5)} < CK = C_{\text{GD}}.$$

A.12. Proof of Corollary 6.5 (Sufficient Conditions for Greedy Multiscale to be Better). From Lemma 6.4, we know greedy multiscale is cheaper than regular projected gradient descent in this setting. We need to show the upper bound on the expected error for regular projected gradient descent (right-hand side of Theorem 6.1) is larger than the corresponding bound for greedy multiscale (right-hand side of Theorem 6.3). Assuming our plan for the number of iterations, $\sum_{t=2}^s K_s = s - 1$ so our bound for greedy multiscale becomes $(q)^{K_1} \sqrt{2^{S+1}} \left((q)^{S-1} + \frac{L_{f^*} |u - \ell|}{2^{S+2} q} \frac{2q - (2q)^S}{1 - 2q} \right)$.

Assume $0 < q < \frac{1}{2}$, and the number of scales S is ≥ 4 and $2^S \geq \frac{L_{f^*} |u - \ell| \sqrt{2}}{2(1-2q)((q)^2 - \sqrt{2}(q)^3)}$. Because $S - 1 \geq 3 > 0$ and $0 < q < 1/2$, we have $1 > 1 - (2q)^{S-1} > 0$. We also have

$$\begin{aligned} \frac{1}{q^2 \sqrt{2^{-1} + 2^{-S}} - q^{S-1}} &\stackrel{(a)}{<} \frac{1}{q^2 \sqrt{2^{-1}} - q^{S-1}} = \frac{q^{-2} \sqrt{2}}{1 - \sqrt{2} q^{S-3}} \\ &\stackrel{(b)}{\leq} \frac{q^{-2} \sqrt{2}}{1 - \sqrt{2} q} = \frac{\sqrt{2}}{q^2 - \sqrt{2} q^3}. \end{aligned}$$

We have the inequality (a) since $2^{-S} > 0$, and (b) since $S - 3 \geq 1$ implies $q^{S-3} \leq q$. This gives us

$$\begin{aligned} 2^S &\geq \frac{L_{f^*} |u - \ell| \sqrt{2}}{2(1-2q)((q)^2 - \sqrt{2}(q)^3)} \\ \text{(by } 1 > 1 - (2q)^{S-1} \text{ and (b)) } \quad 2^S &> \frac{L_{f^*} |u - \ell| (1 - (2q)^{S-1})}{2(1-2q)(q^2 \sqrt{2^{-1} + 2^{-S}} - q^{S-1})} \\ (q^2 \sqrt{2^{-1} + 2^{-S}} - q^{S-1}) 2^S &> \frac{L_{f^*} |u - \ell| (1 - (2q)^{S-1})}{2(1-2q)} \\ q^2 \sqrt{2^{-1} + 2^{-S}} &> q^{S-1} + \frac{L_{f^*} |u - \ell| (1 - (2q)^{S-1})}{2^{S+1}(1-2q)} \frac{2q}{2q} \end{aligned}$$

$$q^2 \sqrt{\frac{2^S + 2}{2^{S+1}}} > q^{S-1} + \frac{L_{f^*} |u - \ell| (2q - (2q)^S)}{2^{S+2}q(1-2q)}$$

$$q^K \sqrt{2^S + 2} > q^{K-2} \sqrt{2^{S+1}} \left(q^{S-1} + \frac{L_{f^*} |u - \ell| (2q - (2q)^S)}{2^{S+2}q(1-2q)} \right).$$

Since $K_1 = K - 2$, this completes the proof.

A.13. Proof of Lemma 6.6 (Cost of Lazy Multiscale). We assume a similar setup to Lemma 6.4: $C_{\text{GD}} = CK = D(2^S + 1)^p$ as before. Now we compare against lazy multiscale with cost $C_{\text{LM}} = \sum_{s=1}^S C_s K_s$ and $C_s = DI^p$, where $I = 2^{S-s}$ for $1 \leq s \leq S-1$ (decent on free variables only), and $C_S = C3^p$ (start with 3 points). So we have the ratios,

$$\frac{C}{C_s} = \frac{D(2^S + 1)^p}{D(2^{S-s})^p} > \frac{(2^S)^p}{(2^{S-s})^p} = (2^s)^p > 2^s \quad \text{and} \quad \frac{C}{C_S} = \frac{D(2^S + 1)^p}{D3^p} > \frac{(2^S)^p}{3^p} > \frac{2^S}{3}.$$

Performing the same number of iterations $K_s = K'$ at each scale, we have,

$$C_{\text{LM}} = \sum_{s=1}^S C_s K_s \leq C \left(\sum_{s=1}^{S-1} 2^{-s} K_s + 2^{-S} 3 K_S \right)$$

$$\leq CK' \left(\sum_{s=1}^{S-1} 2^{-s} + 2^{-S} 3 \right) = CK' (1 - 2^{-S} 2 + 2^{-S} 3) = CK' (1 + 2^{-S}).$$

To ensure this is less than CK , we need $K' < \frac{1}{1+2^{-S}} K$. The right side factor is maximized at $S = 2$ on $2 \leq S$, so we can set $K' = \lceil \frac{1}{1+2^{-2}} K \rceil - 1 = \lceil \frac{4}{5} K \rceil - 1$ and ensure that $C_{\text{LM}} < C_{\text{GD}}$.

A.14. Proof of Corollary 6.8 (Sufficient Conditions for Lazy Multiscale to be Better). From Lemma 6.6, we know lazy multiscale will be cheaper than regular projected gradient descent. It remains to show that the bound on the error at the final scale for lazy multiscale on the right-hand side of (6.3) is less than bound for regular projected gradient descent (6.1).

Let $C = L_{f^*} |u - \ell| / 2$, $h = 1 + q^{K'}$, and $g = q^{-K/5-1}$. To ensure first line below is valid, we cannot have $\sqrt{2}/h = 1$. Otherwise, the logarithm in the denominator becomes zero. Moreover, we assume $K > 5(\log_q(\sqrt{2} - 1) - 1)/4$ so that $\sqrt{2}/h > 1$ and we can write inequality (1) below ensuring $\log(\sqrt{2}/h) > 0$.

$$S \geq \log \left(\frac{g}{h} \left(2 + C \frac{1}{h\sqrt{2}-1} \right) \right) / \log \left(\frac{\sqrt{2}}{h} \right)$$

$$\log \left(\frac{\sqrt{2}}{h} \right) S \stackrel{(1)}{\geq} \log \left(\frac{g}{h} \left(2 + C \frac{1}{h\sqrt{2}-1} \right) \right)$$

$$\sqrt{2^S} \geq gh^{S-1} \left(2 + C \frac{1}{h\sqrt{2}-1} \right)$$

$$\sqrt{2^S + 2} \stackrel{(2)}{>} gh^{S-1} \left(2 + C \frac{1 - (\sqrt{2}h)^{-(S-1)}}{h\sqrt{2}-1} \right)$$

$$q^K \sqrt{2^S + 2} > q^{4K/5-1} \left(2h^{S-1} + C \frac{h^S \sqrt{2^S - h\sqrt{2}}}{\sqrt{2^S} h (h\sqrt{2}-1)} \right)$$

$$q^K \sqrt{2^S + 2} \stackrel{(3)}{>} q^{\lceil 4K/5 \rceil - 1} \left(2h^{S-1} + C \frac{h^S \sqrt{2^S - h\sqrt{2}}}{\sqrt{2^S} h (h\sqrt{2}-1)} \right)$$

$$q^K \sqrt{2^S + 2} > q^{K'} 2(1 + q^{K'})^{S-1} + q^{K'} \frac{L_{f^*}}{2} |u - \ell| \frac{(1+q^{K'})^S \sqrt{2^S - (1+q^{K'})\sqrt{2}}}{\sqrt{2^S} (1+q^{K'}) (\sqrt{2}(1+q^{K'}) - 1)}$$

For inequality (2), we use the fact that $\sqrt{2^S + 2} > \sqrt{2^S}$ and $0 < 1 - (\sqrt{2}h)^{-(S-1)} < 1$ to relax the previous line. For inequality (3), we use the fact that $0 < q < 1$ so that possibly multiplying by at most a factor of q only makes the right-hand side smaller.

**SUPPLEMENTARY MATERIALS: MULTIPLE SCALE METHODS
FOR OPTIMIZATION OF DISCRETIZED CONTINUOUS FUNCTIONS***

NICHOLAS J. E. RICHARDSON[†], NOAH MARUSENKO[‡], AND
MICHAEL P. FRIEDLANDER^{†‡}

SM1. Notation and Definition Reference.

SM1.1. Functional Analysis.

DEFINITION SM1.1 (Gradient). *The gradient $\nabla f : \mathbb{R}^{I_1 \times \dots \times I_N} \rightarrow \mathbb{R}^{I_1 \times \dots \times I_N}$ of a (differentiable) function $f : \mathbb{R}^{I_1 \times \dots \times I_N} \rightarrow \mathbb{R}$ is defined entry-wise for a tensor $A \in \mathbb{R}^{I_1 \times \dots \times I_N}$ by*

$$\nabla f(A)[i_1, \dots, i_N] = \frac{\partial f}{\partial A[i_1, \dots, i_N]}(A).$$

DEFINITION SM1.2 (Lipschitz Function). *A function $g : \mathcal{D} \subseteq \mathbb{R}^{I_1 \times \dots \times I_N} \rightarrow \mathbb{R}^{J_1 \times \dots \times J_M}$ is L_g -Lipschitz when*

$$\|g(A) - g(B)\|_F \leq L_g \|A - B\|_F, \quad \forall A, B \in \mathcal{D}.$$

We call the smallest such L_g the Lipschitz constant of g .

DEFINITION SM1.3 (Smooth Function). *A differentiable function $f : \mathcal{D} \subseteq \mathbb{R}^{I_1 \times \dots \times I_N} \rightarrow \mathbb{R}$ is \mathcal{S}_f -smooth when its gradient $g = \nabla f$ is $L_g = \mathcal{S}_f$ -Lipschitz,*

$$\|\nabla f(A) - \nabla f(B)\|_F \leq \mathcal{S}_f \|A - B\|_F, \quad \forall A, B \in \mathcal{D}.$$

A useful fact is that the sum, composition, and (if also bounded) product of Lipschitz functions are also Lipschitz.

LEMMA SM1.4 (Product of Lipschitz Functions). *Let $f, g : \mathcal{D} \subseteq \mathbb{R}^{I_1 \times \dots \times I_N} \rightarrow \mathbb{R}$ be L_f and L_g Lipschitz respectively. Also assume f and g are bounded with $f(A) \leq \|f\|_\infty$ and $g(A) \leq \|g\|_\infty$ for all $a \in \mathcal{D}$. Then the product function $(fg)(A) = f(A)g(A)$ is Lipschitz with constant*

$$L_{fg} = L_f \|g\|_\infty + L_g \|f\|_\infty.$$

Proof. Let $f, g : \mathcal{D} \rightarrow \mathbb{R}^{I_1 \times \dots \times I_N}$, and $A, B \in \mathcal{D}$.

$$\begin{aligned} |f(A)g(A) - f(B)g(B)| &= |f(A)g(A) - f(A)g(B) + f(A)g(B) - f(B)g(B)| \\ &\leq |f(A)| |g(A) - g(B)| + |g(B)| |f(A) - f(B)| \\ &\leq |f(A)| L_g \|A - B\|_F + |g(B)| L_f \|A - B\|_F \\ &\leq \|f\|_\infty L_g \|A - B\|_F + \|g\|_\infty L_f \|A - B\|_F \\ &= (\|f\|_\infty L_g + \|g\|_\infty L_f) \|A - B\|_F \quad \square \end{aligned}$$

We can extend Lemma SM1.4 to tensor-valued functions $f, g : \mathcal{D} \subseteq \mathbb{R}^{I_1 \times \dots \times I_N} \rightarrow \mathbb{R}^{J_1 \times \dots \times J_M}$ given any product $f \times g : \mathcal{D} \rightarrow \mathbb{R}^{K_1 \times \dots \times K_P}$ that is bilinear,

$$\begin{aligned} f \times (tg + sh) &= t(f \times g) + s(f \times h) \\ (tf + sg) \times h &= t(f \times h) + s(g \times h), \end{aligned}$$

*This work was funded by the Natural Sciences and Engineering Research Council of Canada. Manuscript Date: March 3, 2026.

[†]Department of Mathematics, University of British Columbia, Vancouver, BC, Canada

[‡]Department of Computer Science, University of British Columbia, Vancouver, BC, Canada

for all $t, s \in \mathbb{R}$, and ensures the Frobenius norm is sub-multiplicative,

$$\|f(A) \times g(B)\|_F \leq \|f(A)\|_F \|g(B)\|_F.$$

The functions f and g must still be bounded with

$$\|f(A)\|_F \leq \sup_{A \in \mathcal{D}} \|f(A)\|_F = \|f\|_\infty < \infty,$$

and similarly with g .

SM1.2. Convex Analysis.

DEFINITION SM1.5 (Convex Function). *A function $f : \mathcal{D} \subseteq \mathbb{R}^I \rightarrow \mathbb{R}$ is convex when*

$$f(\lambda x + (1 - \lambda)y) \leq \lambda f(x) + (1 - \lambda)f(y),$$

for all $0 \leq \lambda \leq 1$ and $x, y \in \mathcal{D}$.

When f is differentiable, f is convex when

$$f(y) \geq f(x) + \langle \nabla f(x), y - x \rangle$$

for all $x, y \in \mathcal{D}$.

DEFINITION SM1.6 (Strongly Convex Function). *A function $f : \mathcal{D} \subseteq \mathbb{R}^I \rightarrow \mathbb{R}$ is μ_f -strongly convex for $\mu_f > 0$ when $g(x) = f(x) - \frac{\mu_f}{2} \|x\|_2^2$ is convex.*

When f is differentiable, f is μ_f -strongly convex when

$$f(y) \geq f(x) + \langle \nabla f(x), y - x \rangle + \frac{\mu_f}{2} \|x - y\|_2^2$$

for all $x, y \in \mathcal{D}$.

The vector space \mathbb{R}^I in Definitions SM1.3 and SM1.6 and (2.3) can be extended to tensor spaces $\mathbb{R}^{I_1 \times \dots \times I_N}$ with the Frobenius inner product $\langle X, Y \rangle_F$ and norm $\|\cdot\|_F$ more generally.

SM2. Motivating Example Details. This section explains additional details for the motivating example from subsections 2.1 and 2.3.

For Figure 1, we compare total runtime for $S = 3, 4, \dots, 12$, which yields finest discretizations with $I_1 = 2^S + 1$ points. We initialize by uniformly discretizing the polynomial $p(t) = -2.625t^4 - 1.35t^3 + 2.4t^2 + 1.35t + 0.225$ on $[-1, 1]$ to obtain the initial density approximation $x_S[i] = f(t_S[i])\Delta t_S$ at the coarsest scale. At each scale $s > 1$, we perform one ($K_s = 1$) iteration; at the finest scale ($s = 1$), and we iterate until the objective is within 5% of its optimal value. We generate Legendre measurements for $m = 1, \dots, 5$ using the measurement operator A_1 from subsection 2.1 and add 5% Gaussian noise to obtain y . The regularization parameter $\lambda = 10^{-4}$ balances data fidelity against smoothness.

For Figure 2, we run the motivating example with $2^{10} + 1$ points at the finest scale $s = 1$. The top-left plot shows every 25th iterate k starting with the initialization at $k = 0$ and ending at $k = 250$ when running projected gradient descent at the finest scale ($s = 1$). The top-right plot shows every 250th iterate k , ending with the final iterate $k = 4988$ which satisfies the stopping criteria $\hat{\mathcal{L}}_1(x_1^k) < 0.00024$. The bottom-left plot shows x_s^k at each scale from the coarsest scale $s = 10$ to the second finest $s = 2$, and the iterate at the finest scale $s = 1$ after $k = 25$ iterations. We can make a fair comparison between x_1^{25} on the top-left and bottom-left plots since they

are both the result of running $k = 25$ iterations of projected gradient descent at the finest scale. Using multiscale results in a smoother iterate since x_1^0 was constructed from the chain of interpolations, rather than the completely random initialization used by the single scale approach. Because of this, the bottom-left plot highlights multiscale only needs $k = 387$ iterations at the finest scale to also achieve the same stopping criteria $\tilde{\mathcal{L}}_1(x_1^k) < 0.00024$.

For Figure 3, comparing iterations at different scales is not fair since we expect one projected gradient step to be cheaper at coarser scales. The loss $\tilde{\mathcal{L}}_s(x_s^k)$ for the multiscale method is calculated at the respective scale s of the iterate, whereas the single scale only calculates the the loss $\tilde{\mathcal{L}}_1(x_1^k)$ at the finest scale $s = 1$. This explains why the loss fluctuates up and down during interpolations for coarser scales s when the approximation $\tilde{\mathcal{L}}_s$ for \mathcal{L} is worse. The coarsest scales also take longer than expected because of the additional function call overhead. Despite these drawbacks, multiscale more than makes up for these by reducing the loss significantly faster once iterating on the finer scales. This is make clear by the right plot in Figure 3.

It could be argued that for optimal convergence rates with a first order method, we should not be using a fixed stepsize based on the global Lipschitz constant [SM8]. Using accelerated methods would almost certainly accelerate convergence and not require almost 5000 iterations. But any sort of acceleration could also be used to speed up convergence for the multiscale method which already has a leg-up since the fine scale iterations start closer to the solution.

SM3. Additional Density Unmixing with Tucker-1 Tensor Factorization Details.

SM3.1. Tucker-1 Tensor Decomposition. A tensor decomposition is a factorization of a tensor into multiple (usually smaller) tensors, that can be recombined into the original tensor. Section 7 uses the Tucker-1 decomposition defined in Definition SM3.1.

DEFINITION SM3.1 (Tucker-1 Decomposition). *A rank- R Tucker-1 decomposition of a tensor $Y \in \mathbb{R}^{I_1 \times \dots \times I_N}$ produces a matrix $A \in \mathbb{R}^{I_1 \times R}$, and core tensor $B \in \mathbb{R}^{R \times I_2 \times \dots \times I_N}$ such that*

$$(SM3.1) \quad Y[i_1, \dots, i_N] = \sum_{r=1}^R A[i_1, r] B[r, i_2, \dots, i_N]$$

entry-wise or more compactly,

$$Y = B \times_1 A.$$

Tensor decompositions are not necessarily unique. It should be clear that scaling one factor by $c \neq 0$ and dividing another by c yields the same original tensor. Furthermore, slices can be permuted without affecting the the original tensor. Up to these manipulations, for a fixed rank, there exist criteria that ensures their decompositions are unique [SM5, SM6, SM1].

SM3.2. Formulating Density Unmixing as a Tucker-1 Decomposition Problem. In both the synthetic and geological data, the task is to recover mixtures of probability densities. We accomplish this task by formulating a discretized version of the problem as a tensor decomposition problem.

In the case of the synthetic example in subsection 7.2, we have access to the true probability density mixtures. For the real-world example in subsection 7.3, the

continuous probability density mixtures are estimated from sampling using kernel density estimation [SM2, SM4].

We use the 2-norm/Frobenius loss in the formulation of the continuous decomposition problem (7.1), but alternative losses can be used such as the KL divergence and their corresponding discrete versions based on how the error between the data and model are distributed [SM3]. The constraints (7.1a) and (7.1b) ensure each mixture in the model is indeed a probability density function.

We interpret the tensors $Y \in \mathbb{R}_+^{I \times K_1 \times \dots \times K_N}$ and $B \in \mathbb{R}_+^{R \times K_1 \times \dots \times K_N}$ as samples of the underlying continuous probability density functions

$$Y[i, k_1, \dots, k_N] = y_i(x[k_1, \dots, k_N])\Delta x, \text{ and } B[r, k_1, \dots, k_N] = b_r(x[k_1, \dots, k_N])\Delta x,$$

with a uniformly spaced grid¹ $\{x[k_1, \dots, k_N]\} \subset \mathcal{D}$. We scale by the volume element of the grid,

$$\Delta x = \prod_{n=1}^N \Delta_n x = \prod_{n=1}^N (x[1, \dots, 1, \underbrace{2}_{n}, 1, \dots, 1] - x[1, \dots, 1, \underbrace{1}_{n}, 1, \dots, 1]),$$

to ensure the tensors are normalized, $Y \in \Delta_{K_1 \dots K_N}^I$ and $B \in \Delta_{K_1 \dots K_N}^R$. This leads to the convenient notation of switching from integrals to summations when we discretize;

$$1 = \int_{\mathcal{D}} y_i(x) dx \text{ discretizes to } 1 \approx \sum_{k_1, \dots, k_N=1}^{K_1 \dots K_N} Y[i, k_1, \dots, k_N] \Delta x.$$

In higher dimensions when N is large, it can be expensive to compute the full N -dimensional kernel density estimation² for each b_r and memory intensive to store the full N dimensional tensor Y . We can instead approximate the full distribution $y_i : \mathcal{D} \subseteq \mathbb{R}^N \rightarrow \mathbb{R}_+$ as a product distribution of $J = N$ one-dimensional distributions $y_i^j : \mathcal{D}^j \subseteq \mathbb{R} \rightarrow \mathbb{R}_+$:

$$y_i(x) = \prod_{j=1}^J y_i^j(x[j]), \text{ where } \mathcal{D} = \mathcal{D}^1 \times \dots \times \mathcal{D}^J,$$

and similarly with b_r and b_r^j . This lets us discretize the probability density functions as 3rd order tensors regardless of the number of dimensions N ,

$$Y[i, j, k] = y_i^j(x_k^j) \Delta x^j, \text{ and } B[r, j, k] = b_r^j(x_k^j) \Delta x^j,$$

with a 1D grid $\{x_k^j\} \subset \mathcal{D}^j$ for each $j \in [J]$. The constraint on B also gets similarly modified to

$$B \in \Delta_K^{R, J} = \left\{ B \in \mathbb{R}_+^{R \times J \times K} \mid \forall (r, j) \in [R] \times [J], \sum_{k=1}^K B[r, j, k] = 1 \right\}.$$

We use the full 3-dimensional representation of the probability density mixtures for the synthetic data in subsection 7.2, and use the compressed representation of the 7-dimensional mixtures for the real word data in subsection 7.3.

¹If the domain \mathcal{D} is unbounded, we may restrict the domain to the support of y_i , or where $y_i(x) \geq \epsilon$ for some $\epsilon > 0$.

²Despite the existence of fast algorithms for kernel density estimation [SM9], it can still be cheaper to compute N one-dimensional kernel density estimations than one N -dimensional kernel density estimation.

SM3.3. Solution Algorithm. Let

$$f(A, B) := \frac{1}{2} \|B \times_1 A - Y\|_F^2$$

be the objective function we wish to minimize in (7.2). Following Xu and Yin [SM11], the general approach we take to minimize f is to apply block coordinate descent using each factor as a different block. Let A^t be the t th iteration of A and let

$$(SM3.2a) \quad f_A^t(A) := \frac{1}{2} \|B^t \times A - Y\|_F^2$$

$$(SM3.2b) \quad f_B^t(B) := \frac{1}{2} \|B \times A^t - Y\|_F^2$$

be the (partially updated) objective function at iteration t for the factor A , and similarly with B .

Given initial factors A^0 and B^0 , we alternate through the factors and perform the updates

$$(SM3.3a) \quad A^{t+1} \leftarrow P_{\Delta_A^I} \left(A^t - \frac{1}{\mathcal{S}_{f_A^t}} \nabla f_A^t(A^t) \right)$$

$$(SM3.3b) \quad B^{t+1} \leftarrow P_{\Delta_{K_1 \dots K_N}^R} \left(B^t - \frac{1}{\mathcal{S}_{f_B^t}} \nabla f_B^t(B^t) \right)$$

for $t = 1, 2, \dots$ until some convergence criterion is satisfied. In our case, we iterate until the relative error,

$$\frac{\|B^t \times A^t - Y\|_F}{\|Y\|_F},$$

or mean relative error,

$$\frac{1}{I \cdot K_1 \cdot \dots \cdot K_N} \sum_{k_1, \dots, k_N} \frac{|(B^t \times A^t)[k_1, \dots, k_N] - Y[k_1, \dots, k_N]|}{Y[k_1, \dots, k_N]},$$

is less than some specified tolerance δ . In practice to avoid dividing by small entries of Y , we may take the mean relative error only on the subarray of Y where entries are larger than some threshold. Given Y is in the constraint set Δ_K

We choose a stepsize of $\alpha = 1/\mathcal{S}_{f_A^t}$, since it is a sufficient condition to guarantee $f_A^t(A^{t+1}) \leq f_A^t(A^t)$, but other stepsizes can be used in theory [SM7, Sec. 1.2.3]. This choice also agrees with the best stepsize given in Lemma 2.6 since the least-square loss in (SM3.2a) is $\mathcal{S}_{f_A^t}$ -smooth and $\mu_{f_A^t}$ strongly convex where $\mu_{f_A^t} = \mathcal{S}_{f_A^t}$. A similar idea holds with B in (SM3.2b).

SM4. Synthetic Data Setup. This section details the data used in subsection 7.2. The main setup is provided here, and the full file can be viewed at `julia_experiments/distribution_unmixing_synthetic.jl` in this paper's GitHub repository [SM10].

```
using Distributions

source1a, source1b, source1c = Normal(4, 1), Uniform(-7, 2), Uniform(-1, 1)
source2a, source2b, source2c = Normal(0, 3), Uniform(-2, 2), Exponential(2)
source3a, source3b, source3c = Exponential(1), Normal(0, 1), Normal(0, 3)

source1 = product_distribution([source1a, source1b, source1c])
source2 = product_distribution([source2a, source2b, source2c])
source3 = product_distribution([source3a, source3b, source3c])

sources = (source1, source2, source3)
```

We generate the following 5×3 mixing matrix

```
p1 = [0.0, 0.4, 0.6]
p2 = [0.3, 0.3, 0.4]
p3 = [0.8, 0.2, 0.0]
p4 = [0.2, 0.7, 0.1]
p5 = [0.6, 0.1, 0.3]

A_true = hcat(p1,p2,p3,p4,p5)'
```

and use it to construct 5 mixture distributions.

```
distribution1 = MixtureModel([sources...], p1)
distribution2 = MixtureModel([sources...], p2)
distribution3 = MixtureModel([sources...], p3)
distribution4 = MixtureModel([sources...], p4)
distribution5 = MixtureModel([sources...], p5)
distributions =
    [distribution1, distribution2, distribution3, distribution4, distribution5]
```

These are discretized into $65 \times 65 \times 65$ sample tensors, and stacked into a $5 \times 65 \times 65 \times 65$ tensor Y . We normalize the 1-slices so that they sum to one.

```
sinks = [pdf.((d,), xyz) for d in distributions]
Y = cat(sinks...; dims=4)
# reorder so the first dimension indexes mixtures
Y = permutedims(Y, (4,1,2,3))
Y_slices = eachslice(Y, dims=1)
correction = sum.(Y_slices) # normalize slices to 1
Y_slices ./= correction
```

The options used for both the single and multi scaled factorization are the following.

```
options = (
    rank=3,
    momentum=false,
    model=Tucker1,
    tolerance=(0.05, 1e-6),
    converged=(MeanRelError, ObjectiveValue),
    do_subblock_updates=true,
    constrain_init=true,
    constraints=[nonnegative!, simplex_rows!],
    stats=[Iteration, ObjectiveValue, GradientNNCone, RelativeError, MeanRelError]
,
    mean_rel_error_tol = 1e-4,
    maxiter=50
)
```

At each scale, the algorithm will continue to iterate until one of the following three occur. The mean relative error is below 5%, the objective value is below 10^{-6} , or 50 iterations have occurred. At this point, the iteration at the next smaller scale will start.

To create Figure 7, we modify the options so that we only use the objective value at the convergence criteria. This allows us to make a fairer comparison between different number of coarse iterations, and the analysis in the paper. The code for this figure can be found in `julia_experiments/distribution_unmixing_synthetic_figures.jl`.

SM4.1. Geological Data Factorization Details. We discretize the densities with $K = 2^{10} + 1 = 1025$ points to obtain an input tensor $Y \in \mathbb{R}_+^{20 \times 7 \times 1025}$ and normalize the depth fibres so that $\sum_{k \in [K]} Y[i, j, k] = 1$ for all $i \in [20]$ and $j \in [7]$.

We run the multiscale factorization algorithm with the following call

```
multiscale_factorize(Y; continuous_dims=3, options...)
```

from `BlockTensorFactorization`. The third dimension is specified as continuous since each depth fibre $Y[i, j, :]$ is a discretized continuous probability density function.

This is compared to the regular factorization algorithm

```
factorize(Y; options...)
```

using the Julia package `BenchmarkingTools`. This runs the algorithm as many times as it can within a default time window. Note that a new random initialization is generated for each run. After running the following,

```
using BenchmarkingTools

# Run each function once so they compile
factorize(Y; options...);
multiscale_factorize(Y; continuous_dims=3,options...);

benchmark1 = @benchmark factorize(Y; options...)
display(benchmark1)

benchmark2 = @benchmark multiscale_factorize(Y; continuous_dims=3,options...)
display(benchmark2)
```

we observe the two benchmarks shown in subsection 7.3.

We run the multiscale and single scale factorization algorithms with the following options.

```
options = (
    rank=3,
    momentum=false,
    do_subblock_updates=false,
    model=Tucker1,
    tolerance=(0.12),
    converged=(RelativeError),
    constrain_init=true,
    constraints=[11scale_average12slices! ∘ nonnegative!, nonnegative!],
    stats=[Iteration, ObjectiveValue, GradientNNCone, RelativeError],
    maxiter=200
)
```

We use the same convergence criteria at each scale and iterate until the relative error between the input Y and our model X is at most 12%, or until 200 iterations have passed. We use 12% because this is roughly the error Graham et. al. observe in the final factorization [SM4], suggesting this is the roughly the smallest amount of error we can expect in this factorization.

REFERENCES

- [SM1] A. BHASKARA, M. CHARIKAR, AND A. VIJAYARAGHAVAN, *Uniqueness of Tensor Decompositions with Applications to Polynomial Identifiability*, in Proceedings of The 27th Conference on Learning Theory, PMLR, 2014.
- [SM2] Y.-C. CHEN, *A tutorial on kernel density estimation and recent advances*, Biostat. & Epidemiol., 1 (2017).
- [SM3] N. GILLIS, *NMF models*, in Nonnegative Matrix Factorization, Data Science, Society for Industrial and Applied Mathematics, 2020.
- [SM4] N. GRAHAM, N. RICHARDSON, M. P. FRIEDLANDER, AND J. SAYLOR, *Tracing Sedimentary Origins in Multivariate Geochronology via Constrained Tensor Factorization*, Math. Geosci., (2025).
- [SM5] T. G. KOLDA AND B. W. BADER, *Tensor Decompositions and Applications*, SIAM Rev., 51.
- [SM6] J. B. KRUSKAL, *Three-way arrays: rank and uniqueness of trilinear decompositions, with application to arithmetic complexity and statistics*, Linear Algebr. its Appl., 18 (1977).
- [SM7] Y. NESTEROV, *Nonlinear Optimization*, in Lectures on Convex Optimization, SOIA, Springer International Publishing.
- [SM8] ———, *Smooth Convex Optimization*, in Lectures on Convex Optimization, Y. Nesterov, ed., SOIA, Springer International Publishing, Cham, 2018.
- [SM9] T. A. O'BRIEN, K. KASHINATH, N. R. CAVANAUGH, W. D. COLLINS, AND J. P. O'BRIEN, *A fast and objective multidimensional kernel density estimation method: fastKDE*, Comput. Stat. & Data Anal., 101 (2016).
- [SM10] N. RICHARDSON, N. MARUSENKO, AND M. P. FRIEDLANDER, *richardson-multiscale-2025*. <https://github.com/MPF-Optimization-Laboratory/richardson-multiscale-2025>, 2025.
- [SM11] Y. XU AND W. YIN, *A Block Coordinate Descent Method for Regularized Multiconvex Optimization with Applications to Nonnegative Tensor Factorization and Completion*, SIIMS, 6 (2013).